energies

MDPI

Article

Numerical Analysis of Aeroacoustic Phenomena Generated by Heterogeneous Column of Vehicles

Władysław Marek Hamiga * and Wojciech Bronisław Ciesielka *

Department of Power Systems and Environmental Protection Facilities, AGH University of Science and Technology, 30-059 Kraków, Poland

* Correspondence: hamiga@agh.edu.pl (W.M.H.); ghciesie@cyf-kr.edu.pl (W.B.C.)

Abstract: The last decade has seen an exponential interest in conventional and unconventional energy issues. This trend has also extended to road transport issues and is driven by expectations to minimize fuel and/or energy consumption and negative environmental impact. In the global literature, much attention is focused on the work of autonomous transport, both passenger and trucks, and on the phenomena of platooning. The paper presents original aerodynamic and aeroacoustic tests of heterogeneous vehicle columns. In the work, models of a car, a van and a truck were built, followed by heterogeneous columns with different distances between the vehicles. Computational fluid dynamics (CFD) methods and two turbulence models, $k-\omega$ shear stress transport (SST) and large eddy simulation (LES), were used in this study. The study enabled the determination of drag coefficients and lift force. Application of the Ffowcs Williams–Hawkings (FW-H) analogy allowed for the determination of the distributions of sound pressure levels generated by moving vehicles and columns of vehicles. In order to verify the developed models, acoustic field measurements were made for the following passages: passenger car, van, and truck. Acoustic pressure level and A-weighted sound level (SPL) were measured in Krakow and in its vicinity. Research has shown that grouping vehicles into optimal columns and maintaining distances between vehicles using modern control systems can result in significant energy savings and reduce harmful emissions to the environment.

Keywords: aerodynamics; aeroacoustics; platoon; fuel; LES; CFD; CAA; FW-H; ITS; IEMS

Citation: Hamiga, W.M.; Ciesielka, W.B. Numerical Analysis of Aeroacoustic Phenomena Generated by Heterogeneous Column of Vehicles. *Energies* **2022**, *15*, 4669. https://doi.org/10.3390/en15134669

Academic Editor: Francesco Castellani

Received: 26 May 2022
Accepted: 23 June 2022
Published: 25 June 2022

1. Introduction

Recently, in Europe, as well as in most of the highly industrialized countries, an exponential interest in the issues of both conventional and unconventional power generation has been observed. This is mainly due to a number of reasons, such as the awareness of depletion of fuel resources, a significant increase in their prices, improvement of energy security and efforts to better protect the natural environment. These reasons determine the search for solutions that can reduce the costs for societies and minimize the impact on the environment at every stage of production, distribution and use of energy. One of the most important branches of the European and world economy is the road transport of goods and people, which is responsible for a significant part of energy consumption as well as its emissions, including the emission of greenhouse gases, contributing to climate change, and the emission of acoustic energy (i.e., noise in the environment). This is especially observed in our country with the huge increase in the number of vehicles, especially in the last three decades.

In Poland, according to the Central Statistical Office [1], since the 1970s, we have been continuously observing the development of motorization, manifested by a systematic increase in the number of vehicles. It accelerated significantly after 1990, when there were 5.3 million passenger vehicles, 1 million goods vehicles and 1.4 million motorcycles on Polish roads. In the following years, there was a systematic growth, and thus: in 2000, there were already 10 million passenger vehicles, 1.9 million goods vehicles, and 1.4 million motorcycles; in 2010, there were already 17.2 million passenger vehicles, 3 million goods

vehicles, and 1 million motorcycles; and finally, in 2020, there were already 25.1 million passenger vehicles, 4 million goods vehicles, and 1.7 million motorcycles. Such a huge increase in the number of vehicles will put Poland in second place in the European Union in 2020 as far as the number of vehicles per 1000 inhabitants is concerned, with the result of 656, just behind Luxembourg, where it is 676. The road infrastructure was also expanded during this period. The total length of all roads in Poland in 2020 was 430.3 thousand km, including 1712.2 km of freeways and 2548.5 km of express roads, and even before Poland's accession to the European Union in 2005, there were 552 km of freeways in Poland and 258 km of express roads. The length of Poland's freeways is comparable to that of such countries as Austria or Belgium but is substantially different from that of Italy—6943 km, Germany—13,141 km, or Spain—15,585 km. Such a great number of vehicles and largely insufficient infrastructure of freeways and expressways poses a challenge in searching for technical solutions aimed at improvement of safety, minimization of energy consumption and reduction in negative environmental impacts in the future. One of them may be combining vehicles in homogeneous and heterogeneous columns.

The reduction in drag force can be achieved by optimizing the shape of the vehicle and using additional body elements. In Elsayed's work [2], three methods are presented to improve the aerodynamics efficiency of a car. The use of an additional horizontal rectangular flap at the end of the roof, modification of the roof by a perforated surface layer, as well as the installation of side, vertical rams at the height of the windows. Respectively, 15.87%, 19.82% and 22.67% reduction in the air drag force was achieved.

In the work of Vedrtanm et al. [3], in order to reduce the drag coefficient, passive systems were used. The flow around the vehicle has been modified by using vortex generators (VG) and rear spoilers. The investigation concerned 26 cases, related to different settings of the wing angle of attack, the use of VG, as well as the direction of the crosswind. In the most favorable configuration, a reduction in the drag coefficient reached up to 68.18%.

Active aerodynamic systems are described in Piechna's work [4]. The presented technologies of intelligent systems are based on adjusting the aerodynamic properties based on the velocity of the vehicle. In addition, information on acceleration, yaw rate, steering angle and brake pressure is also taken into account. The systems are used in order to improve the aerodynamic parameters of the vehicle, reducing the amount of fuel consumption, as well as improving the safety and comfort of driving.

A review of modern methods of reducing air drag force was made by Szodrai [5]. The author presents passive and active systems, improving the aerodynamic efficiency of vehicles. The work focuses on two types of vehicles: hatchback and notchback cars.

A slightly different approach to the aerodynamics of road vehicles is presented in the work of Kurec et al. [6]. The aim of the authors was to analyze the active system that acts as an aerodynamic brake. By using properly arranged plates on the hood and the roof of the passenger car, additional forces were generated on the vehicle. The additional drag force is used for braking the vehicle, while the additional downforce is used to increase the grip. The system presented in this paper has a positive effect on the improvement of driving safety.

Many works are focused on the analysis of the aerodynamic parameters of the homogeneous columns [7–14]. These fleets are mainly formed from heavy-duty trucks because of the great interest of transport companies in reducing costs. Reducing the air drag forces acting on the vehicles has a direct impact on the amount of consumed fuel. This is the main reason why international projects focus on research into truck platoons. The projects on homogeneous convoys include: Energy ITS [15], SCANIA [15], PATH [15,16], KONVOI [17], COMPANION [18], European Truck Platoon Challenge (ETPC). It should be emphasized that heavy road transport accounts for only a small percentage of all cars moving on the roads.

Apart from the aerodynamic analysis of a truck model, the authors will also use passenger car and van models. It will increase the potential to reduce the amount of fuel consumption and thus reduce the amount of harmful gases generated and released into

the environment. Research on heterogeneous columns was carried out, among others, by Schito et al. [19]—analysis of a convoy consisting of hatchback, sedan, van and truck. The set distance between the vehicles was from 0.5 to 3 m, and the speed was 30 m/s. Siemon et al. [20]—a study of a heterogeneous column consisting of four trucks with various loading on the semi-trailer. The column speed was defined as approx. 29 m/s. In the work of Lee et al. [21], an analysis of energy consumption depending on the length of the formed heterogeneous column was carried out. The models of transport vehicles were used, which differed in size from each other. The fleet speed in each of the considered cases was approx. 22.22 m/s. Luo et al. [22]—study for four different vehicles: sedan, multi-purpose vehicle (MPV), sport-utility vehicle (SUV) and van trucks. A CFD simulation process of various configuration of platoons was conducted for inter-vehicle spacing in the range of 4 to 30 m. Based on collected data, the estimation model of the drag coefficient was prepared. The authors used a hybrid algorithm combining the BP neural network (BPNN) and particle swarm optimization (PSO).

The major international projects on a heterogeneous fleet of vehicles include Grand Cooperative Driving Challenge (GCDC) [15] or Safe Road Trains for the Environment (SARTRE) [15,23].

The main sources of road noise are trucks, cars and motorcycles, i.e., vehicles moving on the road with their own propulsion. Noise emitted by a moving car comes from engine and powertrain operation, wheel rolling on the road surface, and other factors such as aerodynamic noise from air turbulence while the car is moving, noise from hitting each other and resonant vibrations of poorly maintained body parts [24]. The level of car noise also increases as a function of increasing speed; at lower speeds while driving in low gears, the noise from the powertrain is dominant, at higher speeds, the main source of noise becomes the rolling of wheels on the road surface, and at very high speeds, aerodynamic noise begins to dominate [25].

Currently, the wave methods and geometrical modeling of the sound field around the sources are used for analysis and synthesis. The finite element method (FEM) and boundary element method (BEM) can be numbered among the methods of the first group. In the second group, we count a ray tracing method, a mirror image source method, a conical beam method and a triangular beam method. In recent years, due to the dynamic development of super computers, it has become possible to perform aerodynamic and aeroacoustics calculations for very complex computer models using CFD. As part of the work carried out for several years, the authors have built and verified a simplified car model, which is known in the scientific community as the Ahmed body [26], and a model of a homogeneous column of trucks [27].

The purpose of this work is to create an original, validated numerical model that allows for determining the acoustic field around a column of heterogeneous vehicles to be determined with the lowest weighted drag coefficient. Simulations are based on using the large eddy simulation (LES) turbulence model and the Ffwocs Williams–Hawkings analogy, which are implemented in ANSYS Fluent software. Due to the low Mach number, which was $Ma = 0.075$, the calculations were performed using the Farassant method and presented boundary conditions. The developed model will be used for further research on acoustic and aerodynamic phenomena associated with moving road vehicles and will constitute the so-called "active layer" of the Integrated Management System for Acoustic Environment being developed for the capital and royal city of Krakow by the authors of this work [28–31] and intelligent transport systems (ITSs).

2. Materials and Methods

2.1. Mathematical Model

In the simulation process, the ANSYS Fluent software was used. The aerodynamic parameters connected with airflow around the vehicle were calculated on the basis of the continuity (1) and momentum (2) equations. In accordance with the previous studies [26,27], it was decided to use the $k - \omega$ SST turbulence model for the first stage of the research.

The results were used as initial conditions for transient calculations with the large eddy simulation (LES) turbulence model. Using the Ffowcs Williams–Hawkings Equation (3), the acoustic fields around the selected column of vehicles are calculated. For the performed simulations, it was assumed that the fluid is viscous, Newtonian and incompressible. The effect of gravity has been ignored.

Continuity equation:

$$\nabla \cdot u = 0 \tag{1}$$

Momentum equation:

$$\rho_p \frac{du}{dt} = -\nabla p + \nabla \cdot \tau_{ij} \tag{2}$$

where:

u—air velocity vector
p—pressure
ρ_p—air density
τ_{ij}—stress tensor

Ffowcs Williams–Hawkings equation:

$$\frac{1}{c_0^2}\frac{\partial^2 p'}{\partial t^2} - \nabla^2(\rho') = \frac{\partial^2}{\partial x_i \partial x_j}[T_{ij}H(f)] + \frac{\partial}{\partial t}[Q_n\delta(f)] + \frac{\partial}{\partial x_i}[L_i\delta(f)] \tag{3}$$

where:

$$T_{ij} = \rho u_i u_j + P_{ij} - c_0^2(\rho - \rho_0)\delta_{ij}$$
$$Q_n = \rho_0 v_n + \rho(u_n - v_n)$$
$$L_i = P_{ij}n_j + \rho u_i(u_n - v_n)$$
$$P_{ij} = p\delta_{ij} - \mu_p\left[\frac{\partial u_i}{\partial x_j} + \frac{\partial u_j}{\partial x_i} - \frac{2}{3}\frac{\partial u_k}{\partial x_k}\delta_{ij}\right]$$

u_i—fluid velocity component in the x_i direction
u_n—fluid velocity component normal to the surface f
v_i—surface velocity component in the x_i direction
v_n—surface velocity component normal to the surface f
T_{ij}—lighthill turbulence stress tensor
P_{ij}—compressible stress tensor
$H(f)$—heaviside function
$\delta(f)$—Dirac delta function
δ_{ij}—Kronecker delta
c_0—speed of the sound
ρ'—density fluctuation.

The pressure fluctuation p' is used to calculate the Sound Pressure Level (SPL) L_{sp} according to Equation (4).

$$L_{sp} = 20log_{10}\frac{p'}{p_{ref}}[dB] \tag{4}$$

where:

$p_{ref} = 2 \times 10^{-5}(Pa)$—reference acoustic pressure
p'—pressure fluctuation.

The drag coefficient C_d is calculated according to Equation (5) on the basis of the forces of viscosity and pressure acting on the vehicles.

$$C_d = \frac{2F_d}{\rho_p A u^2} \tag{5}$$

where:

F_d—acting drag force
A—frontal area of the vehicle
u—relative air velocity.

The drag and lift coefficient of the whole heterogeneous column is calculated using weighted arithmetic mean (WAM), presented in Equations (6) and (7).

$$C_{d,WAM} = \frac{C_{d,i}A_i + C_{d,j}A_j + C_{d,k}A_k}{A_i + A_j + A_k} \tag{6}$$

$$C_{l,WAM} = \frac{C_{l,i}A_i + C_{l,j}A_j + C_{l,k}A_k}{A_i + A_j + A_k} \tag{7}$$

where:

A_i, A_j, A_k—frontal area of different vehicles
C_i, C_j, C_k—drag and lift coefficients of different vehicles.

2.2. Geometry Model

The subjects of the research are road vehicles represented by three types of body: a passenger car, a van and a truck. In the presented work, the developed geometries will be used to simulate single cars as well as convoys consisting of three different vehicles. In all three geometric models, the main features related to the shape of the body were reflected. In order to reduce the number of elements and improve the quality of the computational grid related to the model discretization process, some simplifications have been made. Mirrors, antennas and wheel arches were omitted. Modeling of the car chassis, cooling and exhaust systems were abandoned.

The vehicle representation of the passenger car is an Audi A3 from 1998. The catalog value of the drag coefficient for this vehicle is 0.31. The geometric computer model is shown in Figure 1a, while its overall dimensions are shown in Figure 1b.

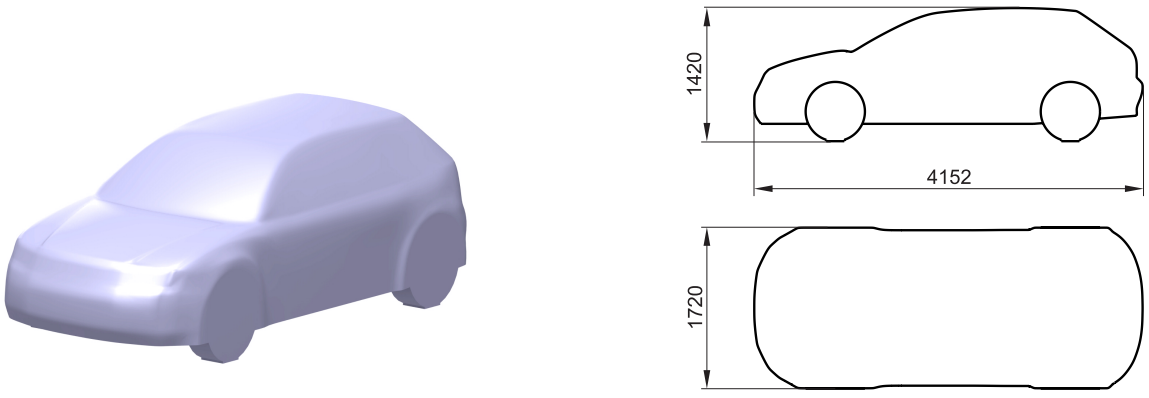

(**a**) (**b**)

Figure 1. (**a**) Isometric view of the passenger car model geometry (**b**) Nominal dimensions of the car model.

The van is a Fiat Ducato, model L3H2. The length of the vehicle is 6 m. The drag coefficient for this model from 2014 is 0.31. The geometric model is shown in Figure 2a, while the overall dimensions are in Figure 2b.

The truck consists of a tractor cab represented by the Mercedes-Benz Actros F, with an additional roof fairing, and a semi-trailer. The total length of the vehicle is 14 m. The value of the drag coefficient of an analogous truck was presented in work [32], and it is about 0.542. The 3D model is shown in Figure 3a, while the overall dimensions are in Figure 3b.

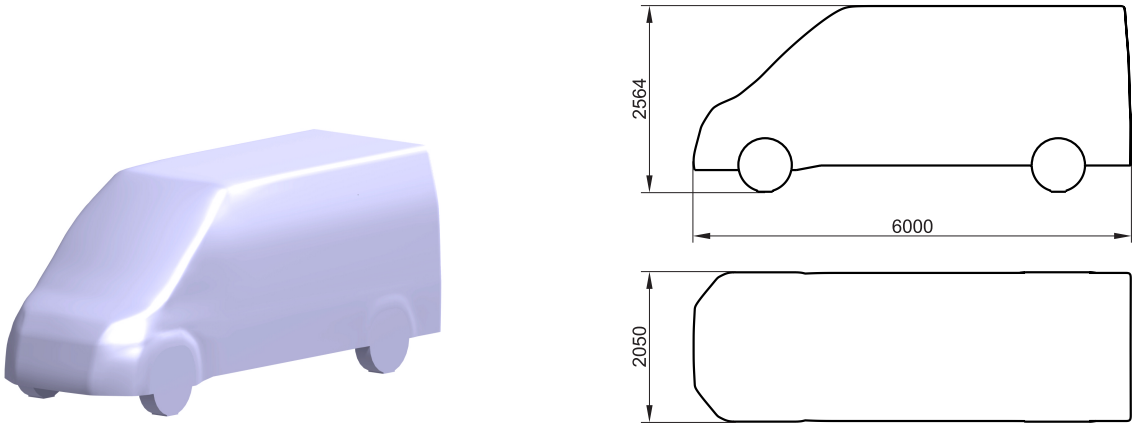

(**a**) (**b**)

Figure 2. (**a**) Isometric view of the van model geometry (**b**) Nominal dimensions of the van model.

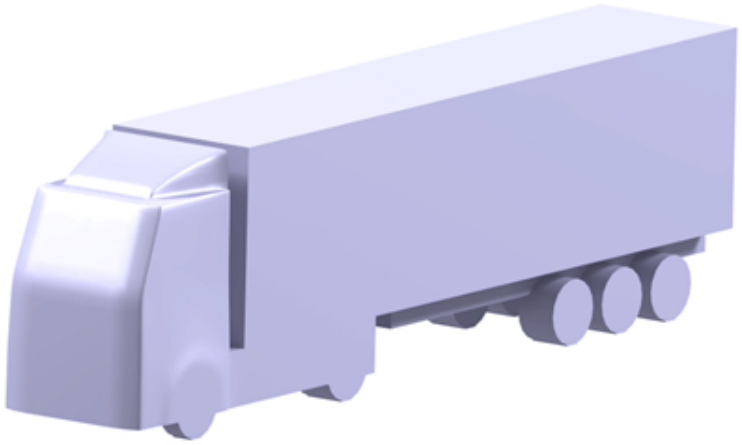

(**a**)

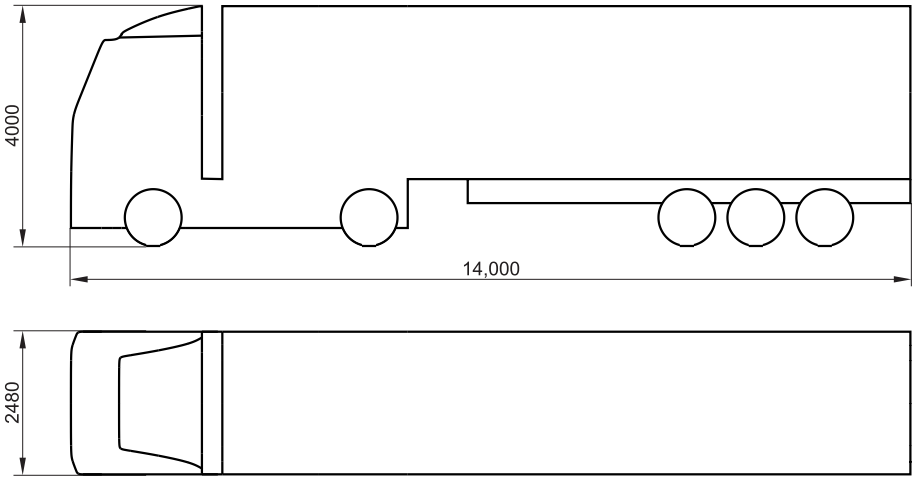

(**b**)

Figure 3. (**a**) Isometric view of the truck model geometry (**b**) Nominal dimensions of the truck model.

2.3. Discretization

Discretization was performed using a structural mesh. The grid parameters were selected on the basis of previous studies presented in [26,27]. The boundary layer around the vehicles consists of 15 elements in height. The height of the first element, expressed by the dimensionless y+ factor, does not exceed 1. A transition layer, consisting of 22 layers, was used between the boundary layer and the rest of the domain. The growth rate parameter for both the boundary layer and transition layer was set to 1.2. Figures 4–6 present the model discretization in the area around the vehicles. The grid is shown from three different views (a–c). Additionally, the mesh detail around the vehicles is shown in d.

The developed model is divided into independent blocks. The first block (enter tunnel) is a 25-m lead-in tunnel. This block contains a boundary condition related to the task of air velocity. The next block is a block with the geometry of the tested vehicle (car tunnel, van tunnel and truck tunnel). The number of elements of vehicle blocks is 18.9 million for the passenger car, 23.92 million for the van, and 54 million for the truck. The minimum value of the orthogonal quality does not fall below the value of 0.1. A distance of 2 m was assumed both in front of and behind the vehicles. In order to assemble a model of a heterogeneous column, three different vehicle's blocks were connected in chosen order. For columns where the distance between the vehicles is 8 and 12 m, middle blocks (middle tunnel) with a length of 4 and 8 m, respectively, were added. The model ends with an end block (end tunnel), which is long for 140 m. Interfaces were used between the blocks. The grid smooths the transition from one block to another (conformal interfaces are used). The exact dimensions, number of elements and the mesh quality of the individual blocks are presented in Table 1.

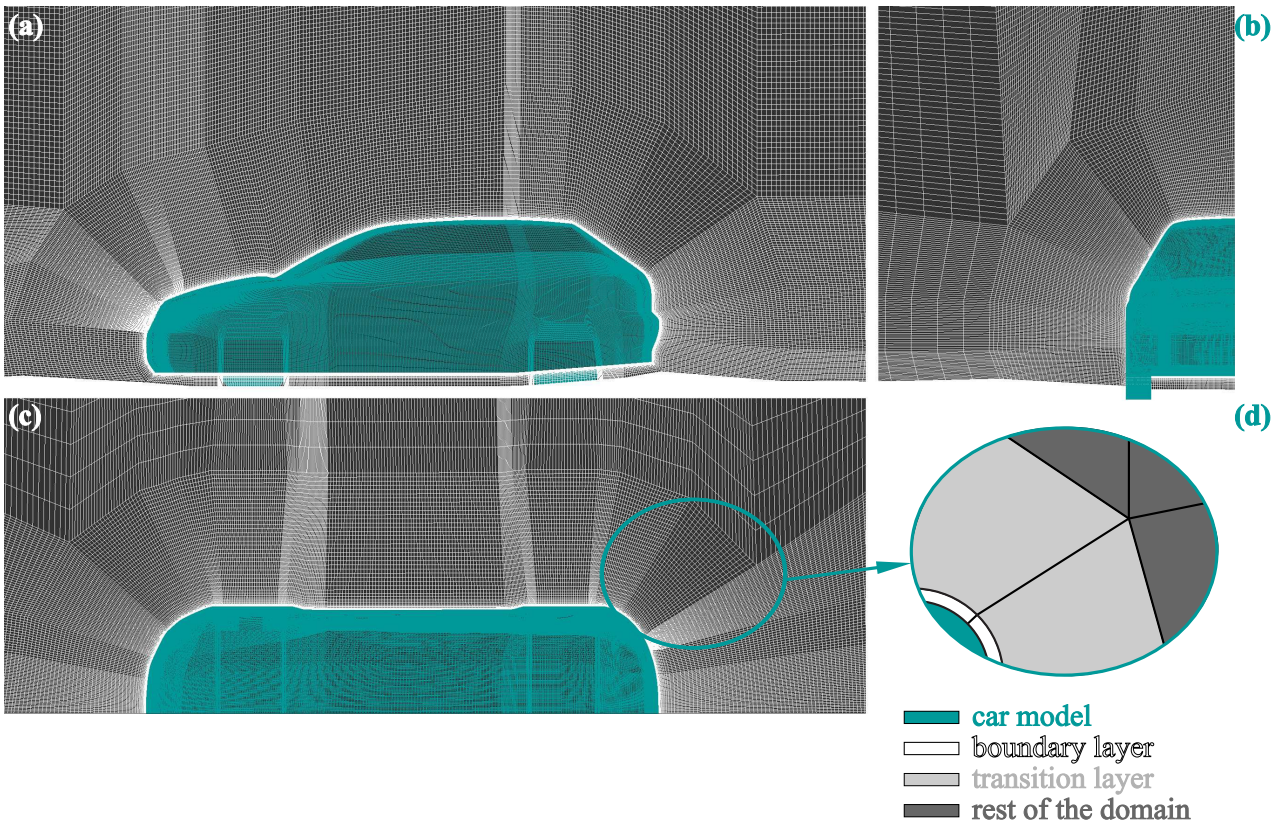

Figure 4. Discretization of single car block—3D model. View from: (**a**) side, (**b**) front, and (**c**) top of the tunnel. (**d**) Schematic of grid layers near the boundary.

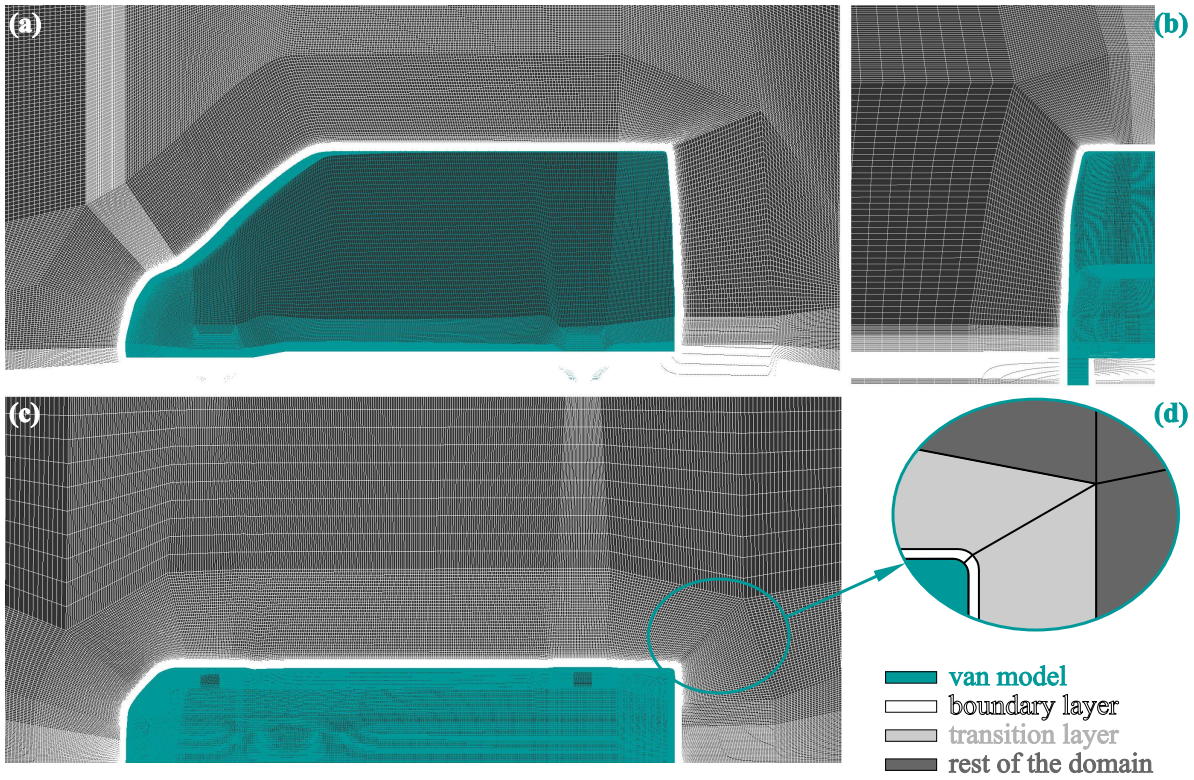

Figure 5. Discretization of single van block—3D model. View from: (**a**) side, (**b**) front, and (**c**) top of the tunnel. (**d**) Schematic of grid layers near the boundary.

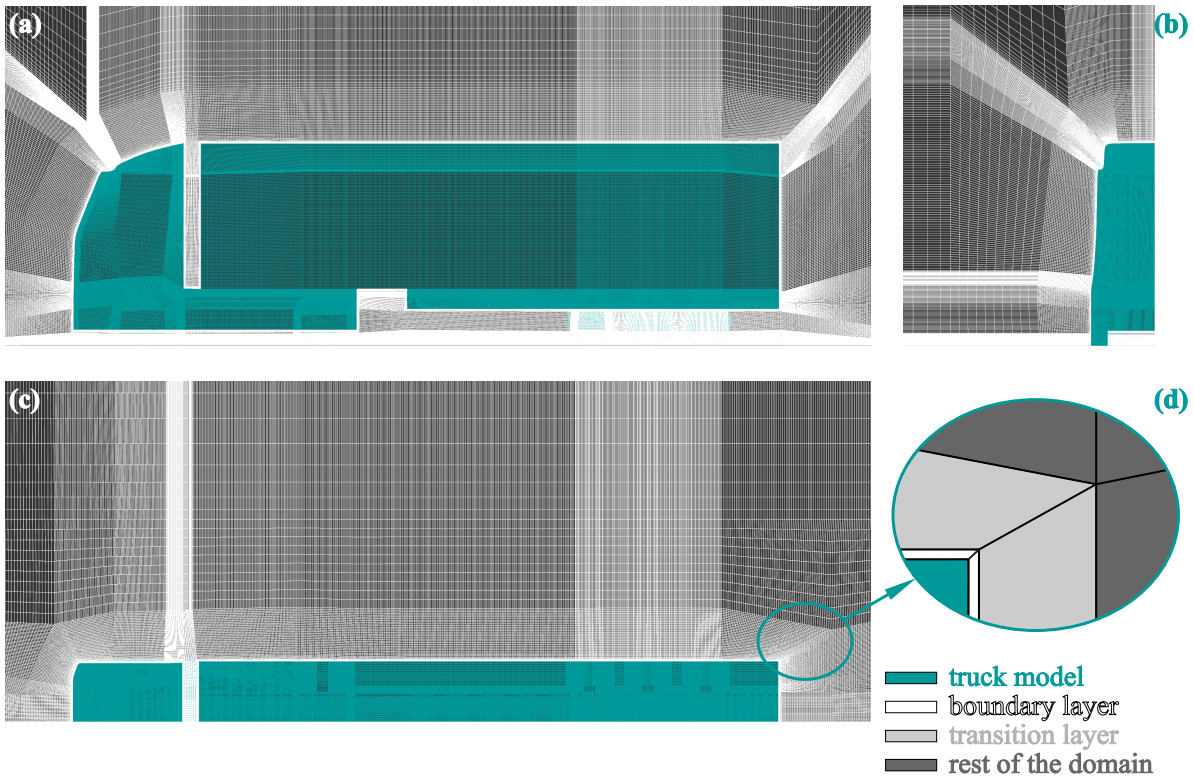

Figure 6. Discretization of single truck block—3D model. View from: (**a**) side, (**b**) front, and (**c**) top of the tunnel. (**d**) Schematic of grid layers near the boundary.

Table 1. Description of mesh blocks.

Block Name	Block Size (m)	Number of Elements $(-) \cdot 10^6$	Minimum Orthogonal Quality $(-)$
Car tunnel	$8.152 \times 8 \times 12$	18.90	0.1
Van tunnel	$10 \times 8 \times 12$	23.92	0.1
Truck tunnel	$18 \times 8 \times 12$	53.95	0.1
Enter tunnel	$25 \times 8 \times 12$	4.09	1
Middle tunnel 4 m	$4 \times 8 \times 12$	3.29	1
Middle tunnel 8 m	$8 \times 8 \times 12$	6.50	1
End tunnel	$140 \times 8 \times 12$	10.51	1

Mesh Independence Study

The mesh parameters were selected on the basis of earlier verification calculations for the simplified geometry of the vehicle known as Ahmed body [26]. On this basis, a computational grid was created for "Car block", "Van block" and "Truck block". The total number of elements for these blocks amounts to 18.9, 23.9 and 54 million, respectively. In order to check whether the calculation result would be independent of the adopted mesh density, it was decided to consider additional models. The new models are associated with local refinement and coarsening of the area around vehicles. The calculations were performed only in the steady state, and the selected parameters and calculation models were applied analogously to those described in this paper.

For passenger car, two coarse meshes and one refined mesh were studied. The difference between the drag coefficient for models "Car_28" and "Car_97" was only 1.27%. Finally, the model "Car_28" was chosen. In the case of the simulation process using coarse meshes for van and truck models, the calculations are divergent. Models "Van_13" and "Truck_18" were rejected. The difference between the base model "Van_33" and the refine model "Van_117" was only 0.35%. For further calculation, the "Van_33" was chosen. Similarly, in the case of the truck, the difference between the base model "Truck_63" and the refine model "Truck_345" was also 0.35%. The "Truck_63" model was chosen.

The results of the calculations and the number of model elements are summarized in Table 2. For further calculation, the authors chose the models highlighted in teal color. The choice of a model with a much smaller number of elements (about five times) allows for a more efficient management of computing resources.

Table 2. Influence of mesh density on aerodynamic parameters.

Model Name	Total Number of Elements $(-) \cdot 10^6$	C_d $(-)$	$C_l(-)$
Car_12	12.30	0.377	0.344
Car_17	17.60	0.321	0.175
Car_28	28.28	0.314	0.138
Car_97	97.70	0.310	0.128
Van_13	13.29	divergence	divergence
Van_33	33.30	0.288	−0.049
Van_117	117.15	0.287	−0.084
Truck_18	17.97	divergence	divergence
Truck_63	63.33	0.572	−0.127
Truck_345	345.47	0.574	–0.132

2.4. Boundary Conditions

Figure 7 shows the computational domain on the example of a heterogeneous column consisting of a van, a truck and a passenger car, respectively. The lower plane (Surface A) is related to the road surface. In the presented models, this surface moves in the opposite direction to the real direction of travel. The absolute speed of this surface is equal to the speed of a column of vehicles. An entry condition is defined on Surface B at the head of the domain. A constant speed of 90 km/h was given. A preliminary disturbance was introduced into the homogeneous air stream, determined by the turbulence intensity parameter I. On the C and D surfaces, the condition of the gradients of all tested parameters was set to zero. The back plane (Surface E) relates to a baseline that has the reference pressure of zero. In order to reduce the number of elements, the symmetry of the model was used. The condition of symmetry was imposed on Surface F. Vehicle bodies are defined by Surfaces G_1, G_2, G_3, with the no-slip condition (speed on the surface of vehicles is equal to zero). The blocks are connected by the $H_1, H_2, \ldots, H_{12}$ surfaces. The numerical mesh on the H surfaces is the same for all modules. A detailed description of the boundary conditions of all surfaces is provided in Equations (A1)–(A26) and attached to Appendix A.

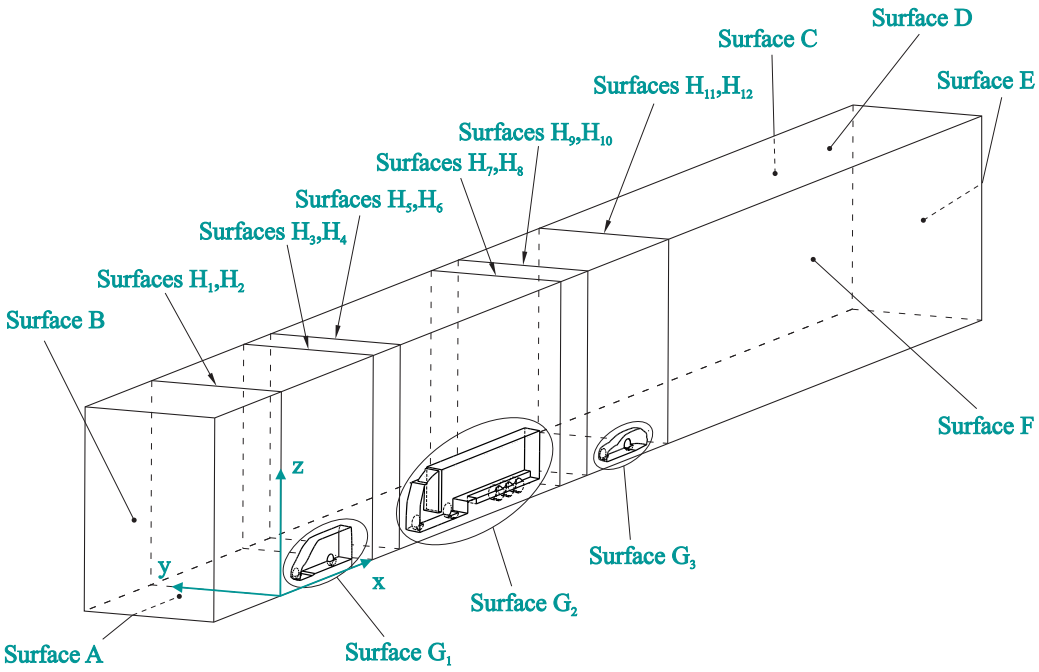

Figure 7. Surface description for boundary conditions on the example of van–truck–car platoon with spacing of 8 m.

2.5. Initial Condition

An initial condition has been defined for the transient calculation. The velocity distribution at the initial moment for $t = 0$ corresponds to the velocity distribution calculated with the Reynolds-Averaged Navier–Stokes (RANS) model (8).

$$\forall_{\substack{a,b,c \in N^+, \\ a \le a_{max}, \\ b \le b_{max}, \\ c \le c_{max}}} \quad u_{a,b,c}(t=0) = u^{k-\omega}_{a,b,c}(t=\infty) \tag{8}$$

where:

a—grid index on the x-axis
b—grid index on the y-axis
c—grid index on the z-axis.

3. Results

3.1. Convergence Criteria

The calculations for the heterogeneous column were performed analogously to those presented in the previous works [26,27]. The simulation was divided into three stages. The first step was to calculate the steady-state using the $k-\omega$ SST turbulence model and the first-order momentum equations. In order to achieve residuals below 10^{-4}, the number of iterations was increased from 100 to 500. The second step of the steady-state calculation uses second-order equations. The assumed residuals below 10^{-4} were reached after 2000 additional iterations. The third stage of the simulation is the transient computation using the LES turbulence model, with time step $\Delta t = 10^{-5}$.

In the case of the numerical model related to a heterogeneous column with inter-vehicle spacing of 4 m, the calculations turned out to be divergent. It was decided to use an additional pressure interpolation scheme. The Body Force Weighted (BFW) schedule was applied to the first 20,000 time steps and then replaced with the recommended Pressure Staggering Option (PRESTO) schedule. For this reason, all tested transient parameters (aerodynamic parameters and acoustic field) are calculated on the basis of the time range of 0.3 to 1 s (from 30,000 to 100,000 time steps) for all three distances. The applied parameters and simulation settings are summarized in Table 3.

Table 3. Convergence criteria, adopted parameters and the mathematical models used for the numerical calculations.

Stage	**I**	**II**	**III**
Convergence criteria	Residuals under 10^{-4}	Residuals under 10^{-4}	Residuals under 10^{-4}
Number of iterations	500	2000	100,000
Turbulence model	$k-\omega$ SST	$k-\omega$ SST	LES
Pressure equation	Second Order	Second Order	Body Force Weighted (BFW) & Pressure Staggering Option (PRESTO)
Momentum equation	First Order	Second Order	Bounded Central Differencing
Relaxation Factor–Pressure	0.25	0.25	0.35
Relaxation Factor–Momentum	0.25	0.25	0.35

3.2. Analysis of Aerodynamic Parameters of a Heterogeneous Column

The amount of used fuel is correlated with the value of aerodynamic forces. Tables 4, 5 and A1–A5 present the results of the analysis, both single vehicles and heterogeneous columns in all of the six possible combinations. Tables A1–A5 are attached to Appendix B. The amount of vehicles are shown in the first table's column. Column number two presents spacing between the vehicles. In column number three, there is information about the vehicle's order in the convoy. For example, in Table 5, the first vehicle in the heterogeneous column is a van, the middle vehicle is a truck, and the last vehicle is a passenger car. Column numbers 4–7 show the value of the calculated aerodynamic parameters. Index "*d*" informs about the drag coefficients, index "*l*" about lift coefficients, index "$k-\omega$" about the use of the $k-\omega$ SST turbulence model, and the index "*LES*" about the use of the Large Eddy Simulation turbulence model. The value of the aerodynamic parameters for transient analysis is calculated using the arithmetic mean. For single vehicles, the used time range is from 0.1 to 1 s, whereas for the heterogeneous columns, it is 0.3 to 1 s. Additionally, for the column of vehicles, the weighted arithmetic mean (WAM) of the drag and lift coefficient is calculated. For this operation, Equations (6) and (7) were used.

The study of aerodynamic parameters starts from the analysis of single vehicles. Table 4 consists of a summary of the drag and lift coefficients for the passenger car, the van and the truck. The simulations are related to the ride of the vehicle in undisturbed airflow.

The most preferable, in terms of reduction in drag force (in two of the three studied spacings), is the heterogeneous column in order: van, truck, passenger car. For the convoy with spacing of 4 m, the value of WAM is 0.337, whereas for a spacing of 8 m, the value of WAM is 0.336. In the case of a spacing of 12 m, the most preferable is the column in order: passenger car, van, truck. The value of WAM is 0.390. In Tables 5 and A2, the preferable values are marked by the color teal.

For the second stage calculation using the LES turbulence model, only one vehicle column was chosen. It was decided to additionally calculate an acoustic parameter for the heterogeneous column: van–truck–car. Because of the limited computational resources, the transient analyses were not performed for the rest of the vehicle convoys. The lack of data in Tables A1–A5 is labeled as "ND" (no data).

Table 4. Drag coefficient and lift coefficient for a single vehicle.

Number of Vehicles $N(-)$	Spacing $S(m)$	Name	$C_{d,k-\omega}$ $(-)$	$C_{d,LES}$ $(-)$	$C_{l,k-\omega}$ $(-)$	$C_{l,LES}$ $(-)$
1	-	Car 1	0.314	0.374	0.138	0.068
1	-	Van 1	0.288	0.308	−0.049	−0.007
1	-	Truck 1	0.572	0.535	−0.127	−0.071

Table 5. Drag coefficient and lift coefficient of vehicles in heterogeneous columns (Van–Truck–Car).

Number of Vehicles $N(-)$	Spacing $S(m)$	Name	$C_{d,k-\omega}$ $(-)$	$C_{d,LES}$ $(-)$	$C_{l,k-\omega}$ $(-)$	$C_{l,LES}$ $(-)$
3	4	Van 1	0.093	0.099	−0.001	0.080
		Truck 2	0.490	0.463	0.007	−0.004
		Car 3	0.1767	0.163	0.026	−0.014
		Weighted arithmetic mean	0.337	0.321	0.008	0.019
3	8	Van 1	0.225	0.247	−0.035	0.008
		Truck 2	0.460	0.463	−0.007	−0.014
		Car 3	0.249	0.286	0.208	0.214
		Weighted arithmetic mean	0.366	0.379	0.011	0.021
3	12	Van 1	0.270	0.296	−0.043	−0.001
		Truck 2	0.495	0.459	−0.039	−0.045
		Car 3	0.322	0.267	0.238	0.210
		Weighted arithmetic mean	0.409	0.388	−0.006	−0.001

The analysis of aerodynamic parameters in the transient state was conducted for a heterogeneous column: van–truck–car. Figures 8–10 show changes in drag and lift coefficients as a function of the number of iterations. The aerodynamic quantities are compared for three vehicle spacings: 4, 8 and 12 m. Figure 8 relates to the vehicle at the head of the convoy (van). The value of the drag coefficient (Figure 8a) decreases with the decreasing distance between the vehicles. This phenomenon is related to the overpressure zone at the front of vehicle number two. For each of the considered cases, the value of the drag coefficient is stable and remains at the level of the values calculated by the steady-state models. Vehicle number one travels in an undisturbed stream of air. For distances of 8 and 12 m, the lift coefficient (Figure 8b) oscillates around the neutral value. At a distance of 4 m, this parameter is unstable and increases to a value of about 0.1 (longer observation of the parameter is required). Lifting force is generated.

Figure 9 shows the parameters related to the vehicle in the center of the column. The truck travels in an airflow disturbed by a van. The forces affecting the vehicle body are highly unstable over time, and the changes reach up to 10%. This is observable both with the drag and lift coefficients. The value of the forces acting on the vehicle is inconclusive and requires averaging.

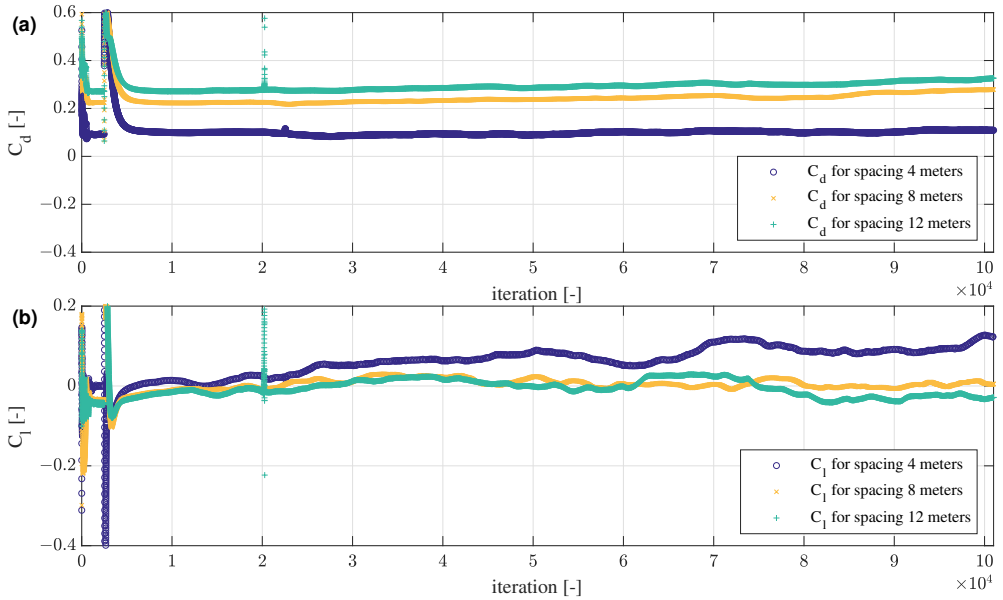

Figure 8. Comparison of the aerodynamic coefficients for heterogeneous columns consisting of three vehicles: van–truck–car. The graph shows data for the first vehicle: van. For the marker: dark blue "o"—the distance between the vehicles is 4 m, orange "×"—the distance between the vehicles is 8 m, teal "+"—the distance between the vehicles is 12 m. (**a**) Drag coefficient. (**b**) Lift coefficient.

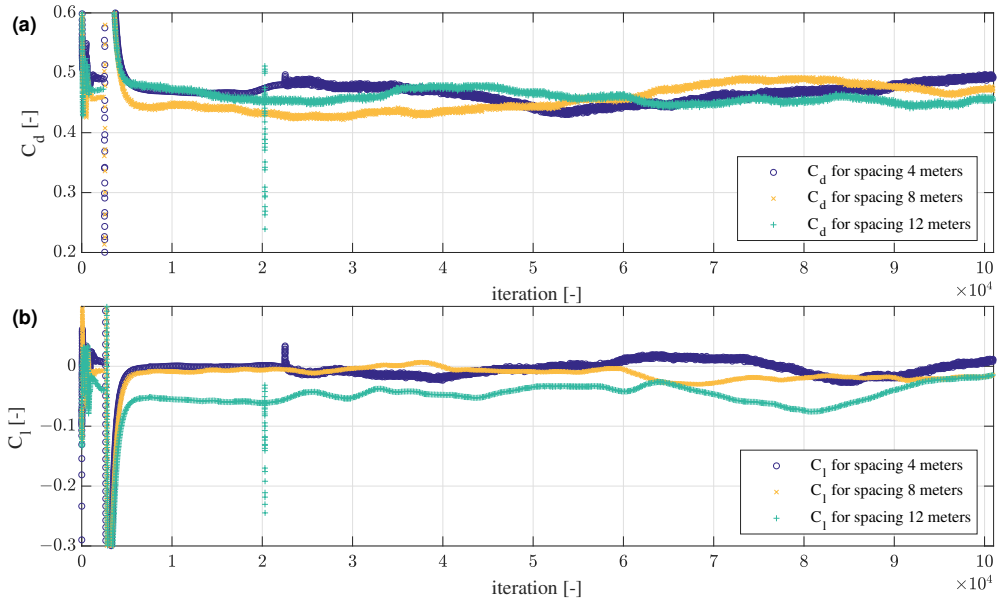

Figure 9. Comparison of the aerodynamic coefficients for heterogeneous columns consisting of three vehicles: van–truck–car. The graph shows the data for the second vehicle: truck. For the marker: dark blue "o"—the distance between the vehicles is 4 m, orange "×"—the distance between the vehicles is 8 m, teal "+"—the distance between the vehicles is 12 m. (**a**) Drag coefficient. (**b**) Lift coefficient.

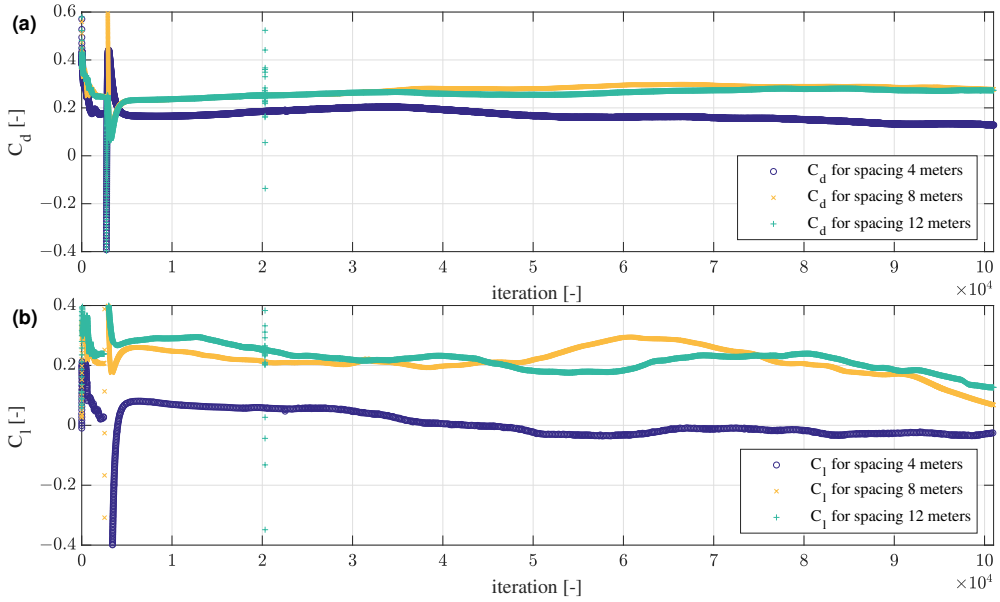

Figure 10. Comparison of the aerodynamic coefficients for heterogeneous columns consisting of three vehicles: van–truck–car. The graph shows data for vehicle number three: car. For the marker: dark blue "o"—the distance between the vehicles is 4 m, orange "×"—the distance between the vehicles is 8 m, teal "+"—the distance between the vehicles is 12 m. (**a**) Drag coefficient. (**b**) Lift coefficient.

Vehicle number three—a passenger car, travels in the wake of the vehicles ahead (Figure 10). The dimensions of a passenger vehicle are several times smaller than that of a truck, which results in the stabilization of aerodynamic parameters. Both the drag force and the lift force decrease with the distance between the vehicles. The value of the drag coefficient for a distance of 4 m is approximately 55% of the value for a single passenger car.

The results of the simulation process of selected quantities in steady-state are presented in Figures 11–14. Figure 11 shows the distribution of the velocity field, Figure 12 concerns streamlines around vehicles, Figure 13 shows pressure distributions, while Figure 14 is related to the dissipation of the kinetic energy of turbulence ω. The analysis is performed on the symmetry plane of the model. Due to the size of the computational domain, only a fragment of the area related to the surroundings of vehicles is presented. Figures 8–10a–c concern the analysis of single-vehicle models in an undisturbed airflow. Figures 8–10d–f are related to the study of a heterogeneous column in the example of a convoy: van–truck–car.

Vehicle number one (van) in front of the column travels in an undisturbed air stream (Figure 14d–f). The pressure distribution in front of the van, shown in Figure 13b, is comparable to the pressure distributions in Figures 13d–f. Behind the vehicle, the situation is different. For a single van, in the zone directly behind the van, the negative pressure is between −100 and −250 Pa (Figure 13b). Two recirculation vortices are formed (Figure 12b). In the case of a vehicle column with a vehicle spacing of 4 m, these eddies directly affect the truck (Figure 12d). The result of this is an increase in pressure field in the area behind vehicle one and a decrease in pressure field in front of vehicle two (Figure 13d). For a heterogeneous column with distances 8 and 12 m (Figure 12e,f), the effect of recirculation vortices is much smaller. Their shape is similar to the structure created behind a single van (Figure 12b). The pressure values are also close to the original distribution. However, the area of influence of the generated wake is much bigger (Figure 11b) and reaches multiples of the vehicle length. This has an impact on the pressure distribution that forms on the front surface of the truck (Figure 12e,f). In the case of a single truck (Figure 13c), the overpressure value is approximately 400 to 500 Pa. For the presented columns, the value of this pressure drops to 50 (Figure 13d), 150 (Figure 13e) and 250 Pa (Figure 13f), depending on the distance between the vehicles. The influence of vehicle number 1 is the dominant factor in reducing the drag coefficient for the vehicle number two. The frontal area of the

passenger car (vehicle number three) is four times smaller and does not affect pressure distribution directly behind the truck (Figure 13d–f). The turbulence area also does not change (Figure 14d–f), relative to the original distribution (Figure 14c). The vehicle at the end of the column is in the wake of vehicle number two (Figure 11d–f). The overpressure zone in front of the vehicle, shown in Figure 11a, is significantly reduced in the case of convoys (Figure 13d–f).

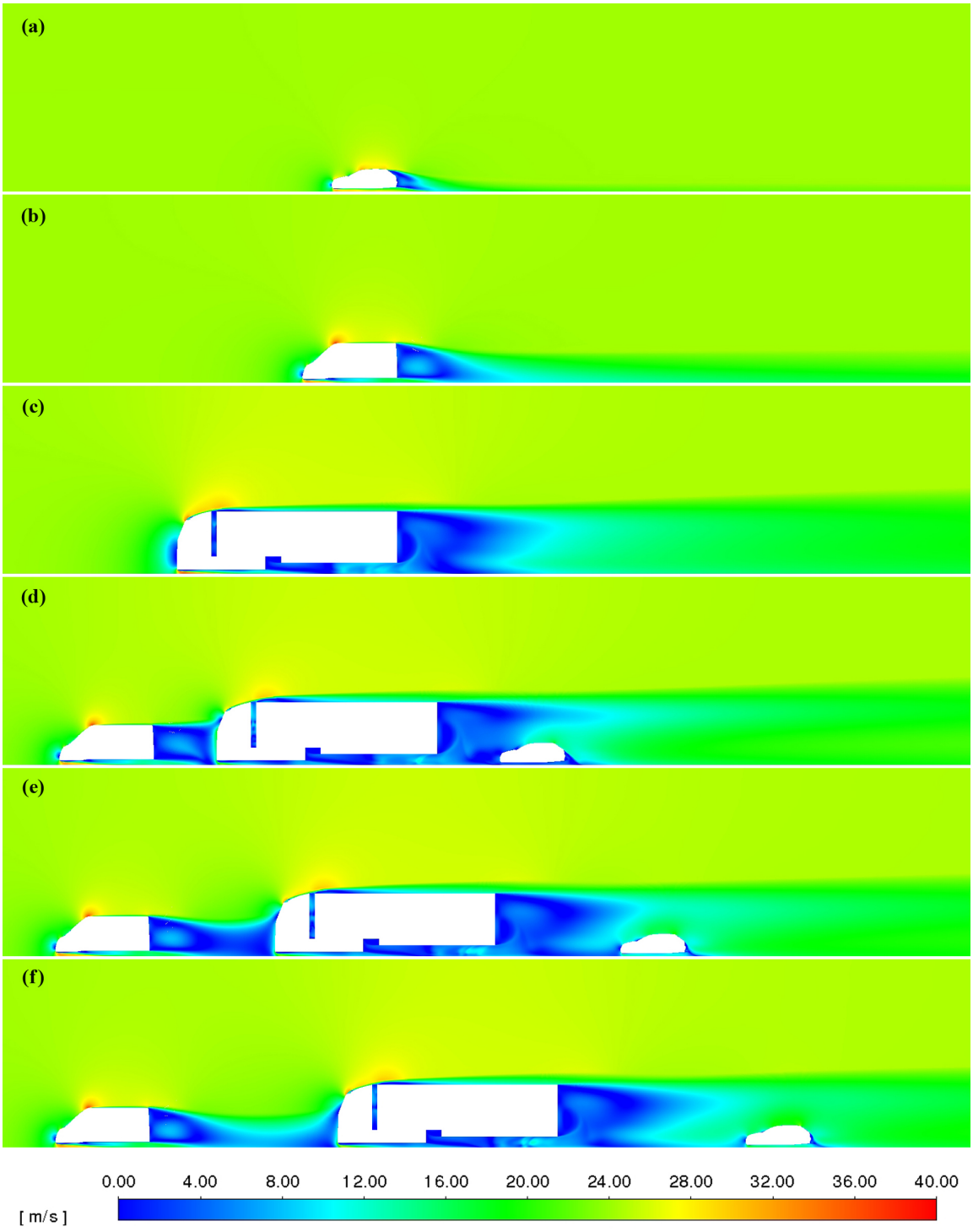

Figure 11. A fragment of velocity filed around the vehicles. View at the symmetry plane. (**a**) Single car, (**b**) single van, (**c**) single truck, (**d**) column of vehicles with a spacing of 4 m, (**e**) column of vehicles with a spacing of 8 m, (**f**) column of vehicles with a spacing of 12 m.

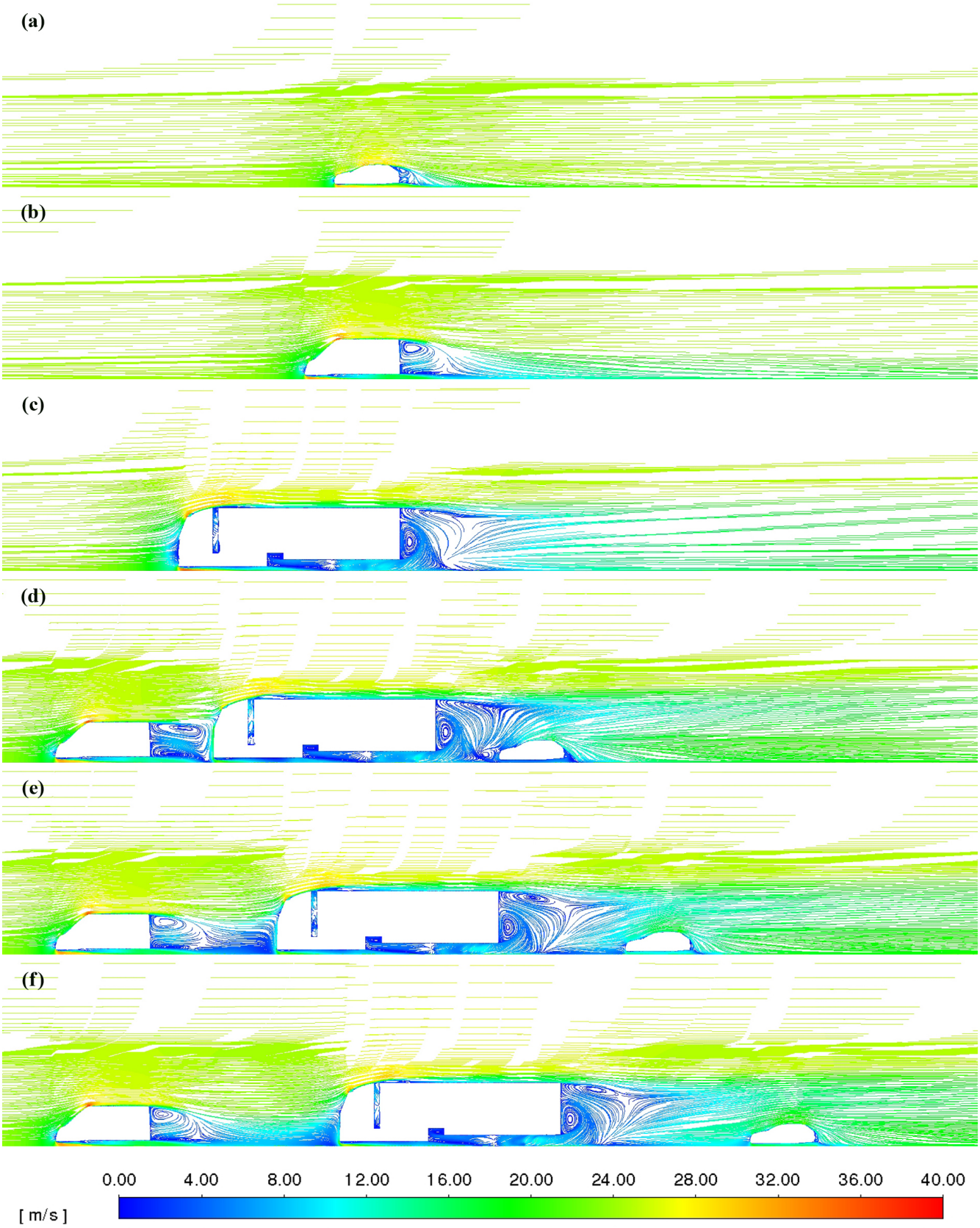

Figure 12. A fragment of streamlines around the vehicles. View at the symmetry plane. (**a**) Single car, (**b**) single van, (**c**) single truck, (**d**) column of vehicles with a spacing of 4 m, (**e**) column of vehicles with a spacing of 8 m, (**f**) column of vehicles with a spacing of 12 m.

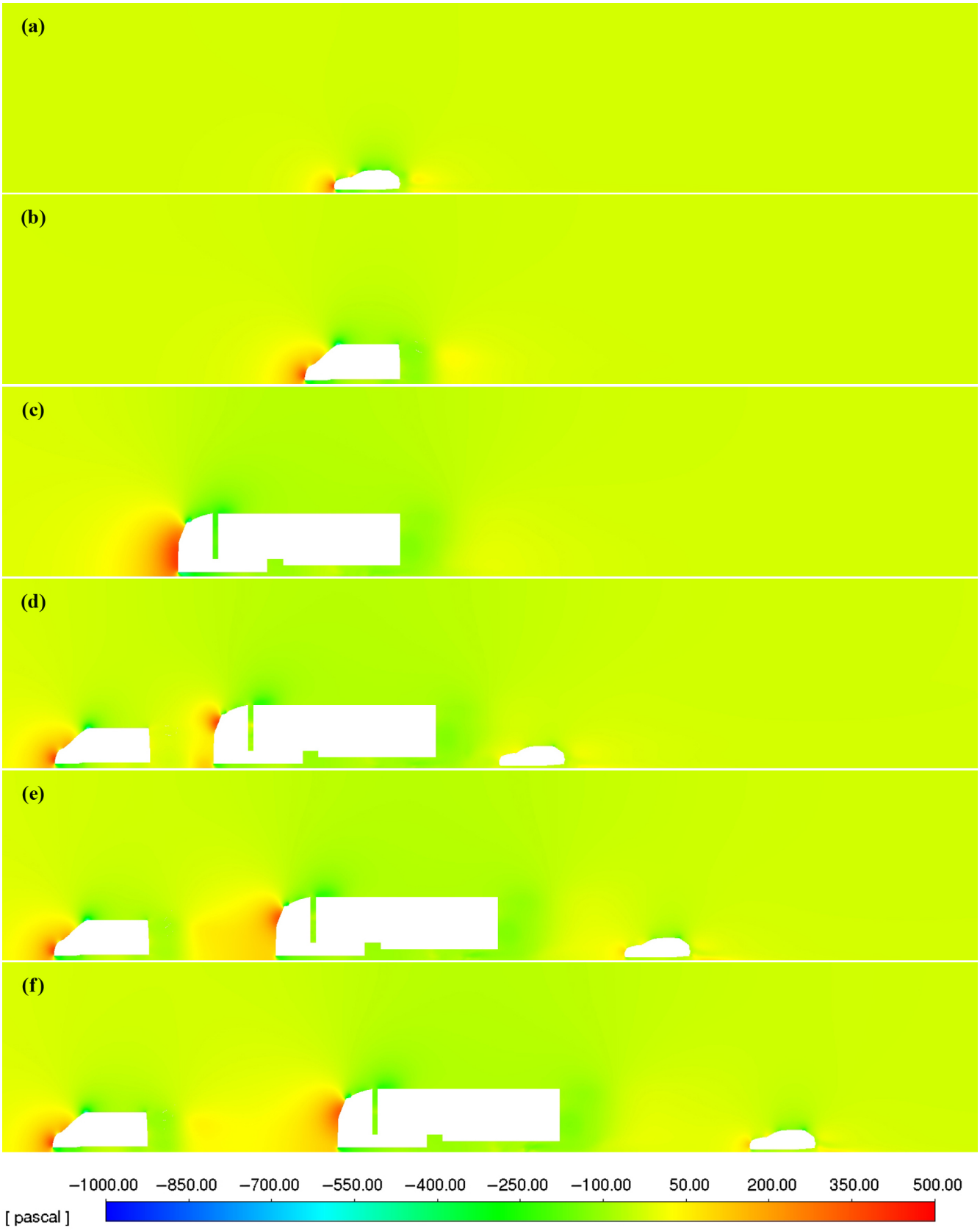

Figure 13. A fragment of pressure distribution around the vehicles. View at the symmetry plane. (**a**) Single car, (**b**) single van, (**c**) single truck, (**d**) column of vehicles with a spacing of 4 m, (**e**) column of vehicles with a spacing of 8 m, (**f**) column of vehicles with a spacing of 12 m.

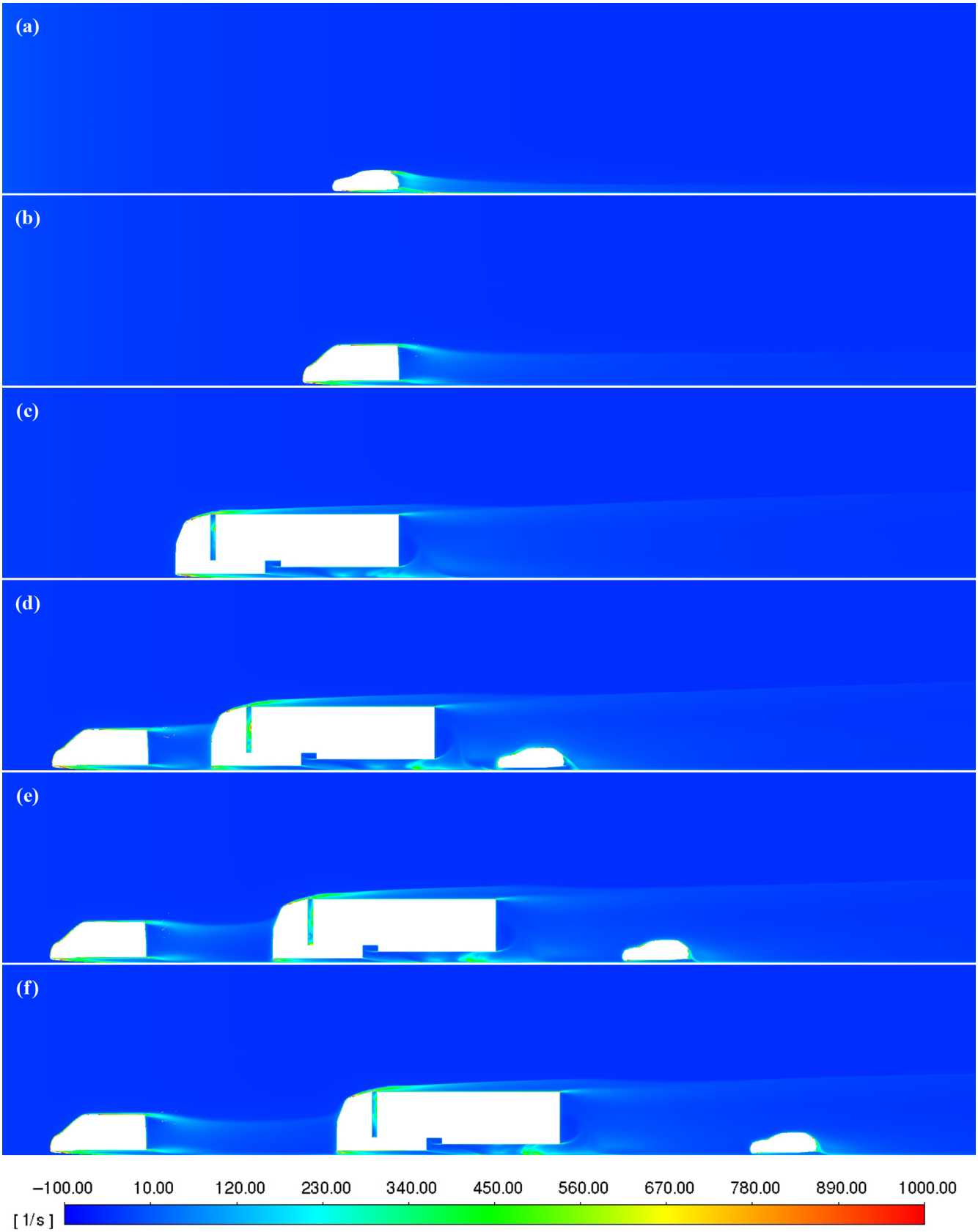

Figure 14. A fragment of turbulence intensity around the vehicles. View at the symmetry plane. (**a**) Single car, (**b**) single van, (**c**) single truck, (**d**) column of vehicles with a spacing of 4 m, (**e**) column of vehicles with a spacing of 8 m, (**f**) column of vehicles with spacing of 12 m.

3.3. Analysis of the Acoustic Field around Individual Vehicles and a Heterogeneous Column

Figures 15–17 present the values of overall sound pressure level determined from the side of the vehicles: passenger car, van and truck. Figures 18–20 present the values of the overall level of acoustic pressure determined from the side for three columns of vehicles with different distances between the vehicles. The vehicle structures are van, truck, and passenger car, respectively. The OASPL values were calculated according to Equation (4), at discrete points 1, 2, and 4 m away from the side surfaces of the vehicles, respectively. The receivers are located at the beginning, middle, and end of each vehicle, at a height of 1.7 m.

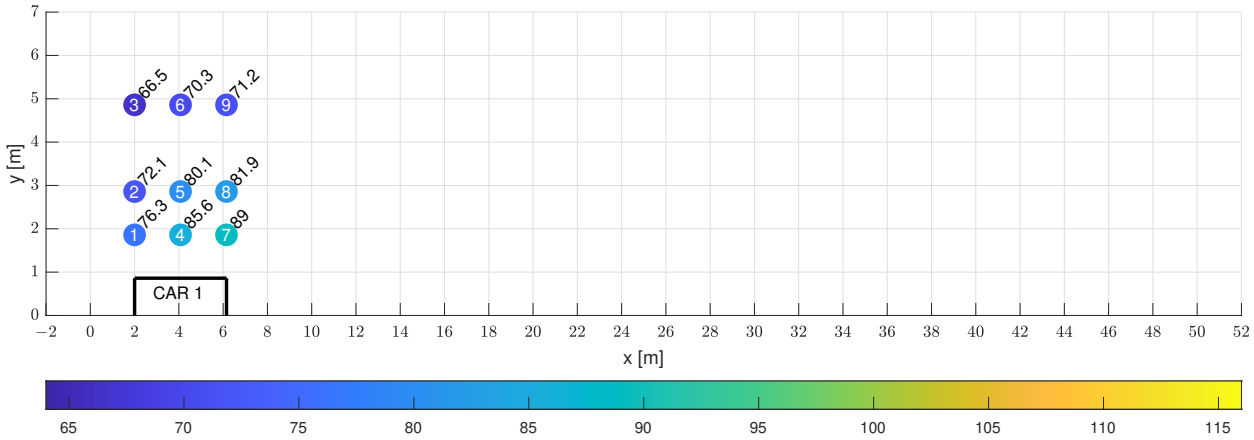

Figure 15. Overall sound pressure level in decibels (dB) on the side of the single car, measured at receivers for the z-coordinate of 1.7 m. View from the top.

For a single passenger car (Figure 15), the highest values of the overall sound pressure level were observed at points 7, 8, 9, i.e., at the third cross-section, while the lowest values were observed at the first cross-section, i.e., points 1, 2, 3. The maximum value of the overall sound pressure level was 89 dB at point 7, i.e., at a distance of 1 m from the vehicle, and the minimum value was 66.5 dB at point 3, at a distance of 4 m from the passenger car. Additionally, the largest difference in overall sound pressure levels was observed between points 7 and 9 and was 17.8 dB, and the smallest difference was 9.8 dB between points 1 and 3.

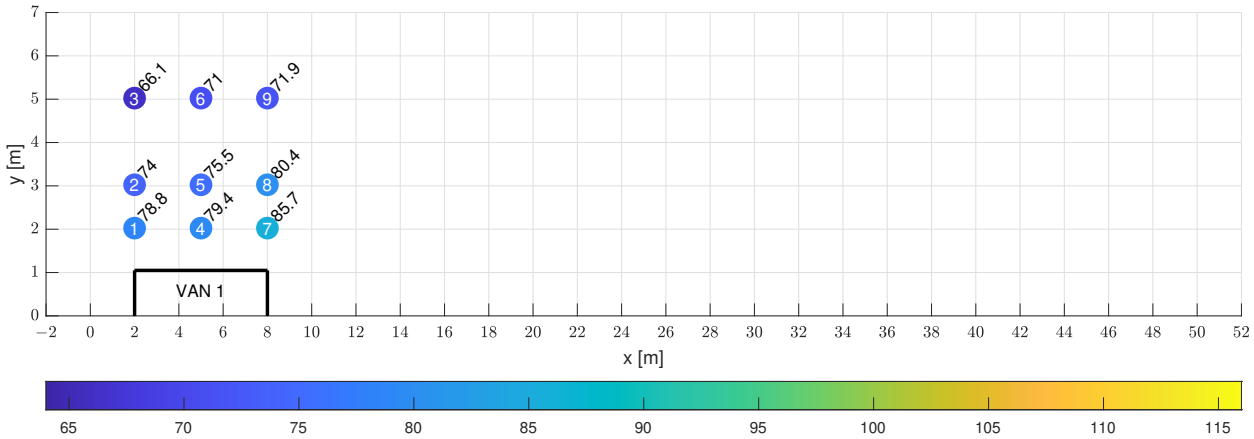

Figure 16. Overall sound pressure level in decibels (dB) on the side of the single van, measured at receivers for the z-coordinate of 1.7 m. View from the top.

For a single van (Figure 16), similarly to a passenger car, the highest values of the overall sound pressure level were observed at points 7, 8, 9, i.e., in the third cross-section, while the lowest values were observed in the first cross-section, i.e., at points 1, 2, 3. The maximum value of the total sound pressure level was 85.7 dB at point 7, i.e., at a distance

of 1 m from the vehicle, and the minimum value was 66.1 dB at point 3, at a distance of 4 m from the passenger car. Additionally, the largest difference in overall sound pressure levels was observed between points 7 and 9 and was 13.8 dB, and the smallest difference was 8.4 dB between points 4 and 6.

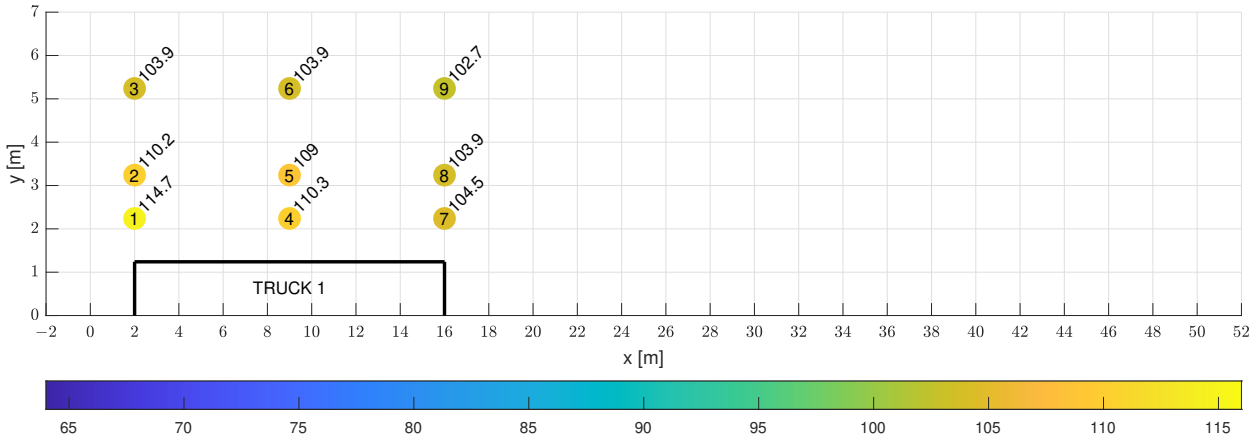

Figure 17. Overall sound pressure level in decibels (dB) on the side of the single truck, measured at receivers for the z-coordinate of 1.7 m. View from the top.

For a single truck (Figure 17), the highest values of overall sound pressure levels were observed at points 1, 2, 3, i.e., at the first cross-section, while the lowest values were observed at the third cross-section, i.e., points 7, 8, 9. The maximum value of overall sound pressure levels was 114.7 dB at point 1, i.e., at a distance of 1 m from the vehicle, and the minimum value was 102.7 dB at point 9, at a distance of 4 m from the truck. Additionally, the largest difference in overall sound pressure levels was observed between points 1 and 3 and was 10.8 dB, and the smallest difference was 1.8 dB between points 7 and 9.

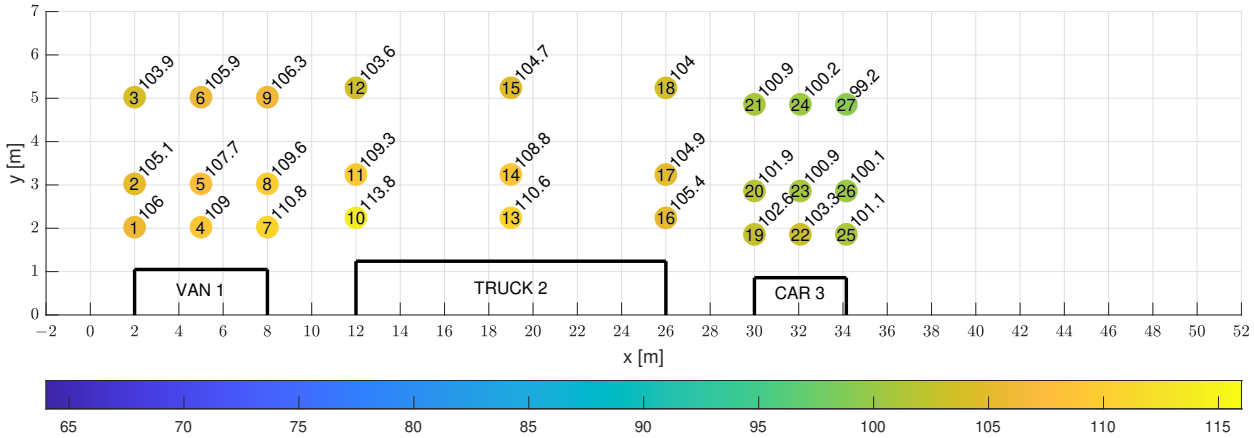

Figure 18. Overall sound pressure level in decibels (dB) on the side of the platoon, measured at receivers for the z-coordinate of 1.7 m. Spacing between trucks: 4 m. View from the top.

Based on the analysis of the results (Figure 18) of the presented distributions of the overall sound pressure levels for the column of cars, we can conclude that at a distance of 1 m from the truck and van, i.e., at points 10, 7, 13, the highest levels occur. The lowest levels of the overall sound pressure level for the distance of 8 m between the vehicles were observed in the last section, i.e., at points 25, 26, 27. In addition, the greatest difference in the overall sound pressure levels was observed between points 10 and 12 and it was 10.2 dB, and the smallest difference was 1.4 dB between points 16 and 18.

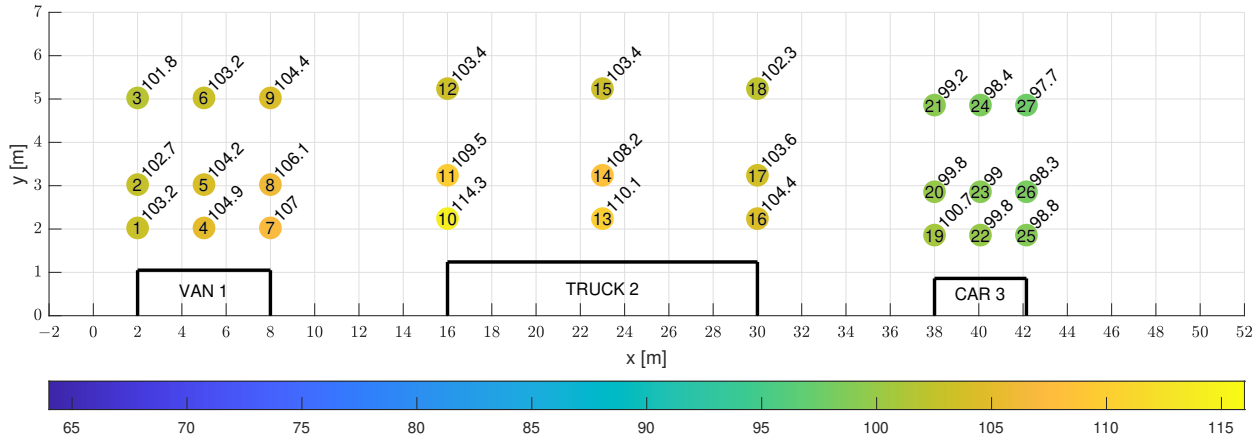

Figure 19. Overall sound pressure level in decibels (dB) on the side of the platoon, measured at receivers for the z-coordinate of 1.7 m. Spacing between trucks: 8 m. View from the top.

On the basis of the analysis of the results (Figure 19) of the presented distributions of the overall sound pressure level for the column of cars, we can state that the highest levels occur at the distance of 1 and 2 m from the truck, i.e., at points 10, 13, 11. The lowest levels of the overall sound pressure level for the distance of 8 m between the vehicles were observed in the last section, i.e., at points 25, 26, 27. Additionally, the biggest difference in the overall sound pressure levels was observed between points 10 and 12 and it was 10.9 dB, and the smallest difference was 1.1 dB between points 25 and 27.

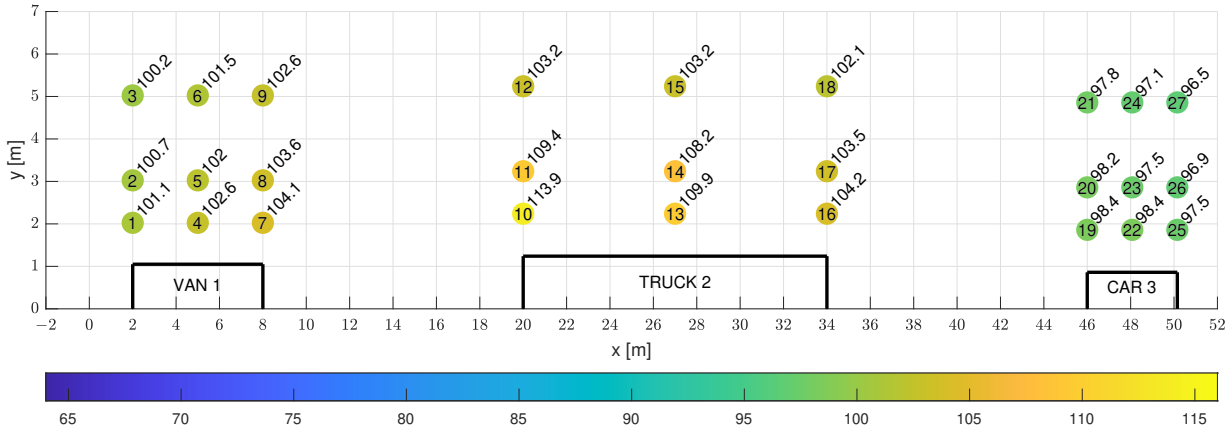

Figure 20. Overall sound pressure level in decibels (dB) on the side of the platoon, measured at receivers for the z-coordinate of 1.7 m. Spacing between trucks: 12 m. View from the top.

On the basis of the analysis of the results (Figure 20) of the presented distributions of the overall sound pressure level for the column of cars, we can state that the highest levels occur at a distance of 1 and 2 m from the truck, i.e., at points 10, 13, 11. The lowest levels of overall sound pressure level for the distance of 12 m between the vehicles were observed in the last section, i.e., at points 25, 26, 27. In addition, the biggest difference in overall sound pressure levels was observed between points 10 and 12 and it was 10.7 dB, and the smallest difference was 0.6 dB between points 19 and 21.

Comparative analysis of the summarized overall sound pressure levels for both single vehicles and car columns showed that the dominant source is a truck. On the other hand, a passenger car and a van are sources that differ in levels by 0.6 and 0.7 dB at a distance of 4 m. Because of the significant differences between the overall sound pressure levels at points in close proximity to individual vehicles and car columns, it was decided to perform additional calculations at a distance of 15 m and a height of 4 m and to determine the

values of the sound pressure level corrected by the A-frequency characteristics. The results obtained are presented later in this article.

3.4. Field Measurements and Computational Verification

In order to confirm the correctness of the calculations carried out, acoustic measurements were conducted in two places in the vicinity of Krakow city. One of them was located at Professor Adam Różanski street and the other one by the Krakow bypass connecting Krakow with the A4 freeway. All measurements were taken at night after 11 p.m. The objects of acoustic tests were a passenger car, a van and a truck. The measurements were made using a sound level meter Svan 945A made by Svantek in windless weather and temperatures of 12 °C to 15 °C. The measurement point at Professor Adam Różanski Street was located 4 m from the source at a height of 1.7 m. Acoustic measurements were taken at this point during the passage of a passenger car and a van. Acoustic measurements for the passage of a truck were made at the Krakow bypass at a distance of 15 m and at a height of 4 m. Apart from measuring the equivalent noise level A for individual vehicles passing at the speed of 90 km/h, the level of the acoustic background was also measured. The test results in the form of spectra in octave bands and equivalent A levels are presented in Figures 21–23.

During the research, the following results of equivalent A levels were registered: L_{Aeq} − 78.7 dB for van, L_{Aeq} − 81.1 dB for passenger car and L_{Aeq} − 81.5 dB for truck.

After conducting field tests, equivalent levels were determined for the previously developed numerical models. Due to the fact that acoustic calculations were performed in time using the finite volume method, the values of equivalent sound level A were determined for a distance of 15 m and a height of 4 m. For a single truck, the result was L_{Aeq} − 81.5 dB. For a heterogeneous column of vehicles and a distance between vehicles of 12 m, the L_{Aeq} value was 79.9 dB. For a column of vehicles and a distance of 8 m, the L_{Aeq} value was 80.4 dB, and for vehicles moving in a column and an inter-vehicle distance of 4 m, the L_{Aeq} was 85.6 dB. Comparing the results of the equivalent sound level A measured and calculated from the model simulation studies using CFD for a single truck, it should be noted that the results are almost identical. In order to verify the obtained results and due to the fact that the authors did not have three exclusive vehicles to perform multivariate field measurements, except for only a passenger car and a rented van, additional calculation methods are recommended for road noise environmental impact assessments [33,34] were applied. The calculations were performed using SoundPlan software. At this stage of the work, four models were developed using the NMPB-Routes-2008 method and ISO 9613-2. These were a single truck model and heterogeneous columns of vehicles with three different distances between vehicles. The study made the following assumptions, which were derived from the dimensions of the vehicles and the distances between them, and then converted to the number of vehicles per hour. A vehicle speed of 90 km/h was assumed in all cases. For a van–truck–car column and a distance of 4 m, it was calculated that there would be 7500 veh/h in the model, for 8 m 5625 veh/h, and for 12 m 4500 veh/h. Trucks accounted for one-third of the total number of vehicles, while passenger vehicles and vans accounted for two-thirds of the total number of vehicles. After entering the data into the model, the calculations were made, and the results of equivalent sound level A were obtained; for single truck L_{Aeq} − 81.6 dB, for column of cars and distance of 4 m L_{Aeq} − 84.0 dB, for 8 m L_{Aeq} − 82.8 dB, and for 12 m L_{Aeq} − 81.8 dB. Analyzing the above presented results for heterogeneous vehicle columns, it should be stated that the differences between the values obtained on the basis of calculation methods, i.e., French method and finite volume method, are within the limits of −1.6 to 2.4 dB, which is a satisfactory result. The differences are mainly due to the failure of the CFD models to consider the dynamic contact between numerous truck tires and the roadway. For a single truck, the equivalent noise level A results differ by 0.1 dB.

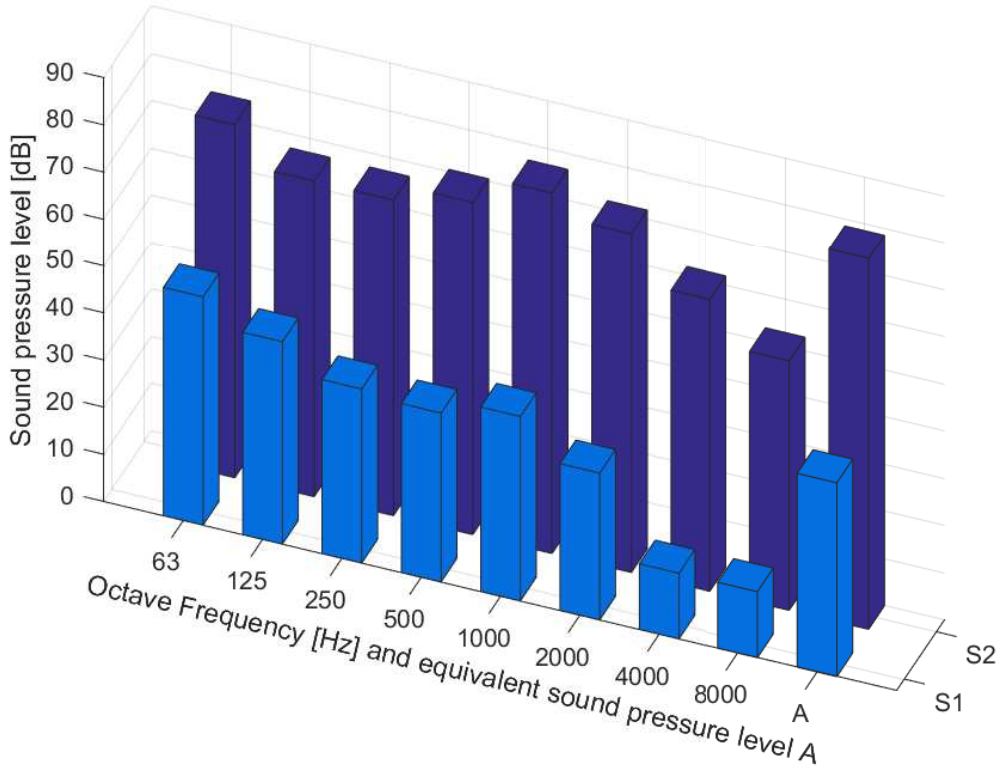

Figure 21. Sound pressure level in octave bands and equivalent sound pressure level A: dark blue—van crossing, light blue—acoustic background.

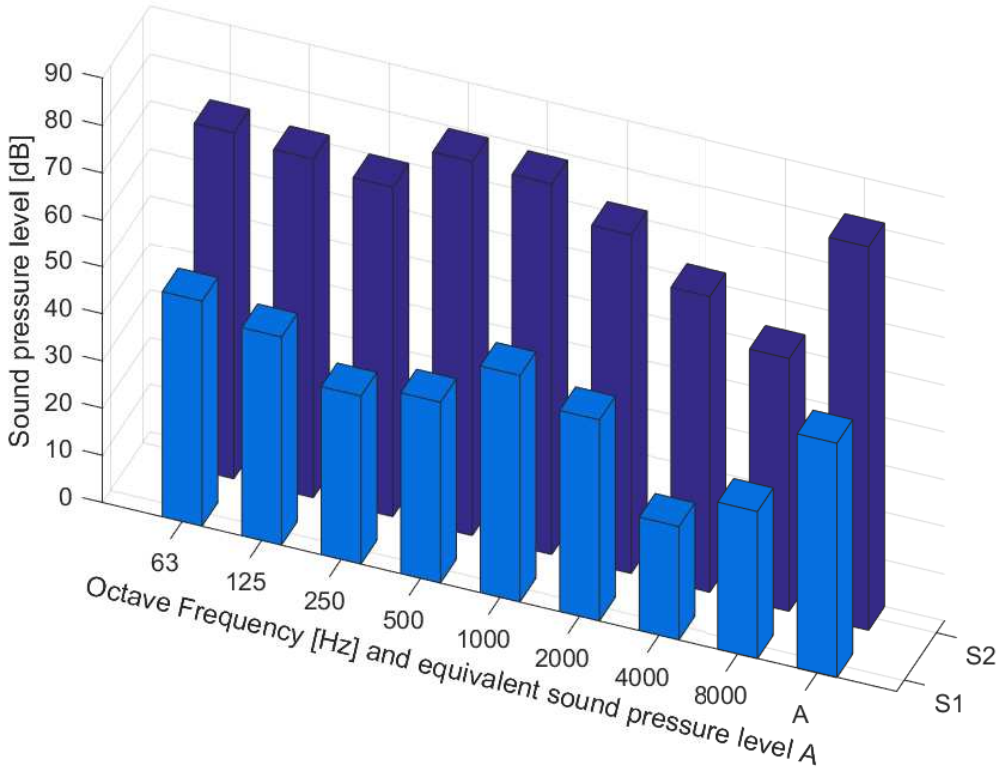

Figure 22. Sound pressure level in octave bands and equivalent sound pressure level A: dark blue—truck crossing, light blue—acoustic background.

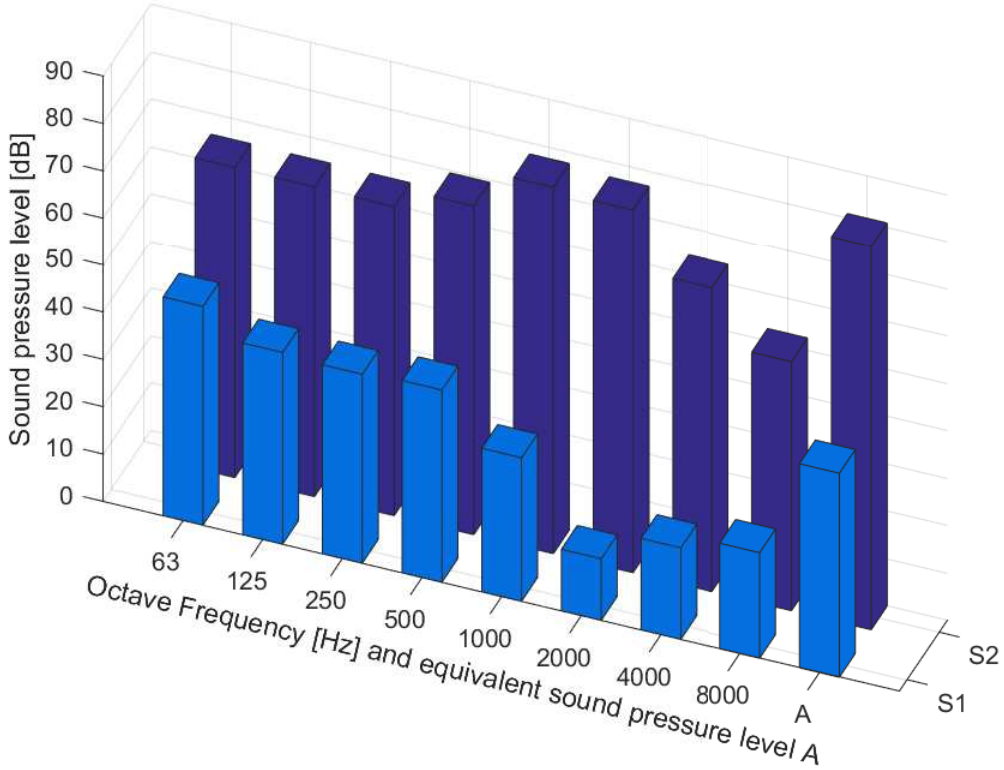

Figure 23. Sound pressure level in octave bands and equivalent sound pressure level A: dark blue—passenger car crossing, light blue—acoustic background.

4. Discussion and Conclusions

The research presented in this paper concerns the analysis of aerodynamic parameters and the acoustic field around heterogeneous columns. The columns consist of three vehicles, represented by three different body types. Small passenger car Audi A3, medium-sized transport van Fiat Ducato car, the L3H2 model and a large truck Mercedes-Benz Actros F tractor with a semi-trailer. These cars were grouped into columns in all of the six possible combinations. Due to the significant reduction in drag coefficients for two of the three tested distances, it was decided to perform further analysis related to the transient state only for the column with the following structure: van, truck, passenger car. The analysis in the unsteady state of the remaining vehicle group structures was not possible due to limited computing resources. The test results showed the aerodynamic parameters of individual vehicles as well as the entire columns. In the second case, the weighted average of the drag coefficient was calculated on the basis of the acting forces and the vehicle's front surface perpendicular to its movement. The distributions of velocity, streamlines around vehicles, pressure field and turbulence kinetic energy dissipation on the plane of symmetry are presented. The total sound pressure level was also calculated at selected points.

The most advantageous column configurations due to the reduction in the drag coefficient is: van, truck, passenger car—for spacing 4 and 8 m, and passenger car, van, truck—for spacing 12 m. The values of the weighted average coefficient of the drag force for these configurations are, respectively, 0.337, 0.366 and 0.390. In all tested vehicle configurations, the value of the weighted average drag coefficient decreases with the decreasing distance between the vehicles. The smallest value of this parameter was calculated for the column: van, truck, passenger car, with a spacing 4 m and it is 0.337. The highest value, equal to 0.437, was achieved for the column: truck, passenger car, van, with a spacing of 12 m. If these vehicles traveled separately, the value of the weighted average drag coefficient would be 0.458. Thus, if the wrong vehicle configuration, convoy velocity and separation between cars were chosen, the overall gain from forming a column of vehicles would be only about

4.6%. For comparison, with the optimal selection of the aforementioned parameters, the drag force reduction reaches up to 26.4%.

Considering the aerodynamics of the vehicle column, the recirculation vortices arising directly behind the vehicles may have a positive effect on the drag force coefficient. This effect applies to vehicles traveling in the wake, by maintaining sufficiently small separation distance. In the case of the presented studies, it is the spacing of 4 m when the vortex from the vehicle in front affects the next vehicle. In further studies, it should be tested with the use of vortex generators. An increase in the recirculation vortex zone could additionally lead to a reduction in drag coefficients for spacing of 8 and 12 m.

The presented research shows the movement of a column of vehicles in an idealized situation in an undisturbed stream of air. In order to estimate the influence of other road vehicles on the aerodynamic parameters of the vehicle column, an additional study should be carried out. The investigation could be performed, for example, by using different turbulence intensities at the inlet and outlet from the computational domain.

Acoustic measurements were made in parallel to the calculation work using CFD. They were conducted in good atmospheric conditions at night in two places in the Krakow agglomeration. A professional class 1 m type Svan 945A made by Polish company Svantek was used in the experiments. Acoustic pressure level and equivalent sound level A were measured for the Audi A3 passenger car, Fiat Ducato van–model L3H2, and Mercedes-Benz Actros F truck with a semi-trailer in the area of Krakow and its surroundings. During the research, the following results of the equivalent sound level A were registered: for a van at the distance of 4 m and 1.7 m height $L_{Aeq} - 78.7$ dB, for a passenger car at the distance of 4 m and 1.7 m height $L_{Aeq} - 81.1$ dB and for a truck at the distance of 15 m and 4 m height $L_{Aeq} - 81.5$ dB. During the works, it was ensured that the vehicles were moving at a constant speed of 90 km/h on the minimum engine power. On the basis of field analyses, it was observed that in the case of a passenger car and a van, the main source of noise is the rolling of tires on the asphalt surface. The difference in noise levels between the passenger car and the van was primarily due to the poorer quality tires used on the passenger car. The acoustic measurements also indicated that the truck was the dominant source of noise. After completing the drag coefficient analyses for individual vehicles and heterogeneous columns, the sound field distributions generated by the moving vehicles were determined. At this stage, Ffowcs Williams–Hawkings (FW-H) analogies were used, and overall sound pressure levels and equivalent A sound levels were determined. Based on the analyses of overall sound pressure levels for individual vehicles, it was found that the dominant source of aerodynamic noise is the truck. The difference in overall sound pressure levels between the truck and the car or van was large at over 30 dB. This was to be expected, especially for the average speed, which was 90 km/h and the drag coefficients, which were for the truck: $C_{d,k-\omega} - 0.572$, $C_{d,LES} - 0.535$, passenger car: $C_{d,k-\omega} - 0.314$, $C_{d,LES} - 0.374$ and van $C_{d,k-\omega} - 0.288$, $C_{d,LES} - 0.308$.

In order to verify the obtained results and due to the fact that the authors did not have three vehicles at their disposal exclusively to perform multivariate field measurements (except for a passenger car and a rented van), additional calculation methods were applied. The method used was NMPB-Routes-2008 and ISO 9613-2 recommended for road noise impact assessments in European Union countries. Calculations were performed using SoundPlan software in which models were built and data were entered for individual vehicles and heterogeneous columns. After calculations, the following results of equivalent sound level A were obtained: for single truck $L_{Aeq} - 81.6$ dB, for a column of cars and distance of 4 m $L_{Aeq} - 84.0$ dB, for 8 m $L_{Aeq} - 82.8$ dB, and for 12 m $L_{Aeq} - 81.8$ dB.

Comparing the results of the equivalent sound level A determined by the French method and finite volume method and the Ffowcs Williams–Hawkings (FW-H) analogy, it was found that they range from -1.6 to 2.4 dB for heterogeneous columns and differ only by 0.1 dB for the dominant source, which is a truck. The numerous tests performed showed the good quality of the built aerodynamic and aeroacoustic models.

Detailed analysis of the applied models allows concluding that in the case of heterogeneous vehicle columns with smaller distances between the vehicles, they will cause increased acoustic energy emission in the short term, but in the daytime or night-time perspective, as long as this phenomenon is not continuous in time, they will cause equal emissions in the environment. In addition, an appropriate configuration of vehicles in a column as shown, van–truck–car, will reduce the drag force by up to 26.4%, which will significantly reduce fuel consumption and, in the future, electricity or hydrogen consumption.

Grouping vehicles into optimal columns and maintaining the distance between vehicles using modern control systems can result in significant energy savings and reduce harmful emissions to the environment. At the same time, continuous work should be performed to minimize the drag coefficients of trucks.

The results presented in this paper are universal and can be used to build intelligent transport systems (ITS) and intelligent environmental management systems (IEMS) for municipalities, counties, cities and urban agglomerations.

Author Contributions: Conceptualization, W.M.H. and W.B.C.; methodology, W.M.H. and W.B.C.; software, W.M.H. and W.B.C.; validation, W.M.H. and W.B.C.; formal analysis, W.M.H.; investigation, W.M.H. and W.B.C.; writing—original draft preparation, W.M.H. and W.B.C.; review, W.B.C.; visualization, W.M.H. All authors have read and agreed to the published version of the manuscript.

Funding: This research received no external funding.

Institutional Review Board Statement: Not applicable.

Informed Consent Statement: Not applicable.

Data Availability Statement: Not applicable.

Acknowledgments: This research was conducted with the support of the PL-Grid (Polish NGI) Consortium, coordinated by the ACC Cyfronet AGH, grant id: plgphdaia. Simulations were performed on the supercomputer Prometheus in the Academic Computer Centre Cyfronet AGH. Each of the numerical simulations in steady-state were solved on 8 nodes and 192 cores. In the presented work, the transient calculations were necessary due to the need to perform the spectral analysis for the heterogeneous column of van–truck–car. These numerical cases were calculated on 10 nodes with a total number of cores of 240. The total used computational wall time exceeded 3,000,000 h. For parallel calculation on Prometheus, additional GPU queue was used. Because of the size of the model, the needed computer memory RAM for post-processing exceeded 600 GB. The geometry models were created in CATIA V5 software. Mesh preparation was conducted in ANSYS ICEM. As a solver, ANSYS Fluent was used. Fast Fourier transform and further calculations and visualizations were made in MATLAB.

Conflicts of Interest: The authors declare no conflict of interest.

Abbreviations

The following abbreviations are used in this manuscript:

SST	Shear Stress Transport
LES	Large Eddy Simulation
FW-H	Ffowcs Williams–Hawkings
ITS	Intelligent Transport System
IEMS	Intelligent Environmental Management Systems
VG	Vortex Generators
SPL	Sound Pressure Level
RANS	Reynolds-Averaged Navier–Stokes
CAA	Computational Aeroacoustics
FFT	Fast Fourier Transformation
MPV	Multi-Purpose Vehicle
SUV	Sport-Utility Vehicle
BPNN	BP Neural Network

PSO	Particle Swarm Optimization
GCDC	Grand Cooperative Driving Challenge
SARTRE	Safe Road Trains for the Environment
FEM	Finite Element Method
BEM	Boundary Element Method
ETPC	European Truck Platoon Challenge
BFW	Body Force Weighted
PRESTO	Pressure Staggering Option
OASPL	Overall Sound Pressure Level

Appendix A. Boundary Conditions

(Surface A) The bottom surface of the channel is defined as a moving wall with constant velocity of 25 m/s:

$$u_x = 25\frac{m}{s}, \quad u_y = 0, \quad u_z = 0 \tag{A1}$$

$$\frac{\partial k}{\partial z} = 0, \quad \frac{\partial \omega}{\partial z} = 0, \quad \nabla p = 0 \tag{A2}$$

$$k_w = \frac{u_\tau^2}{\sqrt{\beta_\infty^*}} \tag{A3}$$

$$\omega_w = \frac{u_\tau}{\kappa y_w \sqrt{\beta_\infty^*}} \tag{A4}$$

for	$S = 4$ m:	$-25\text{ m} \le x \le 176.152$ m,	$0 \le y \le 8$ m,	$z = 0$
for	$S = 8$ m:	$-25\text{ m} \le x \le 184.152$ m,	$0 \le y \le 8$ m,	$z = 0$
for	$S = 12$ m:	$-25\text{ m} \le x \le 192.152$ m,	$0 \le y \le 8$ m,	$z = 0$

where:

k_w—turbulent kinetic energy in the wall cell
ω_w—specific turbulence dissipation in the wall cell
y_w—distance from wall to cell centroid.

(Surface B) At the inlet of the channel, the air velocity is fixed to a constant value 25 m/s:

$$u_x = 25\frac{m}{s} \quad u_y = 0, \quad u_z = 0 \tag{A5}$$

$$\nabla p = 0 \tag{A6}$$

$$k = \frac{3}{2}(u_x I)^2 \tag{A7}$$

$$\omega = \rho_p \frac{k}{\mu_p}\left(\frac{\mu_t}{\mu_p}\right)^{-1} \tag{A8}$$

for	$x = -25$ m,	$0 \le y \le 8$ m,	$0 \le z \le 12$ m

where:

$I = 1\%$—turbulence intensity
$\frac{\mu_t}{\mu_p} = 10$—turbulent viscosity ratio.

(Surface C) The side of the channel is defined as a symmetry:

$$u_y = 0 \tag{A9}$$

$$\frac{\partial u_x}{\partial y} = 0, \quad \frac{\partial u_y}{\partial y} = 0, \quad \frac{\partial u_z}{\partial y} = 0, \quad \frac{\partial p}{\partial y} = 0, \quad \frac{\partial k}{\partial y} = 0, \quad \frac{\partial \omega}{\partial y} = 0 \tag{A10}$$

for	$S = 4$ m:	$-25 \text{ m} \leq x \leq 176.152$ m,	$y = 8$ m,	$0 \leq z \leq 12$ m
for	$S = 8$ m:	$-25 \text{ m} \leq x \leq 184.152$ m,	$y = 8$ m,	$0 \leq z \leq 12$ m
for	$S = 12$ m:	$-25 \text{ m} \leq x \leq 192.152$ m,	$y = 8$ m,	$0 \leq z \leq 12$ m

(Surface D) The top of the channel is defined as a symmetry:

$$u_z = 0 \tag{A11}$$

$$\frac{\partial u_x}{\partial z} = 0, \quad \frac{\partial u_y}{\partial z} = 0, \quad \frac{\partial u_z}{\partial z} = 0, \quad \frac{\partial p}{\partial z} = 0, \quad \frac{\partial k}{\partial z} = 0, \quad \frac{\partial \omega}{\partial z} = 0 \tag{A12}$$

for	$S = 4$ m:	$-25 \text{ m} \leq x \leq 176.152$ m,	$0 \leq y \leq 8$ m,	$z = 12$ m
for	$S = 8$ m:	$-25 \text{ m} \leq x \leq 184.152$ m,	$0 \leq y \leq 8$ m,	$z = 12$ m
for	$S = 12$ m:	$-25 \text{ m} \leq x \leq 192.152$ m,	$0 \leq y \leq 8$ m,	$z = 12$ m

(Surface E) At the outlet of the channel. the pressure is fixed:

$$p = 0 \tag{A13}$$

$$\nabla u = 0, \quad \nabla k = 0, \quad \nabla \omega = 0 \tag{A14}$$

$$k = \frac{3}{2}(u_{avg} I)^2 \tag{A15}$$

$$\omega = \rho_p \frac{k}{\mu_p} \left(\frac{\mu_t}{\mu_p} \right)^{-1} \tag{A16}$$

for	$S = 4$ m:	$x = 176.152$ m,	$0 \leq y \leq 8$ m,	$0 \leq z \leq 12$ m
for	$S = 8$ m:	$x = 184.152$ m,	$0 \leq y \leq 8$ m,	$0 \leq z \leq 12$ m
for	$S = 12$ m:	$x = 192.152$ m,	$0 \leq y \leq 8$ m,	$0 \leq z \leq 12$ m

where:

u_{avg}—mean flow velocity
$I = 5\%$—backflow turbulent intensity
$\frac{\mu_t}{\mu_p} = 10$—backflow turbulent viscosity ratio.

(Surface F) The side of the channel with the vehicles contours is defined as a symmetry:

$$u_y = 0 \tag{A17}$$

$$\frac{\partial u_x}{\partial y} = 0, \quad \frac{\partial u_y}{\partial y} = 0, \quad \frac{\partial u_z}{\partial y} = 0, \quad \frac{\partial p}{\partial y} = 0, \quad \frac{\partial k}{\partial y} = 0, \quad \frac{\partial \omega}{\partial y} = 0 \tag{A18}$$

for	$S = 4$ m:	$-25 \text{ m} \leq x \leq 176.152$ m,	$y = 0$,	$0 \leq z \leq 12$ m
for	$S = 8$ m:	$-25 \text{ m} \leq x \leq 184.152$ m,	$y = 0$,	$0 \leq z \leq 12$ m
for	$S = 12$ m:	$-25 \text{ m} \leq x \leq 192.152$ m,	$y = 0$,	$0 \leq z \leq 12$ m

(Surface G_1, G_2, G_3) The surfaces of the vehicles is defined as a wall with a no-slip condition:

$$u_x = 0, \quad u_y = 0, \quad u_z = 0 \tag{A19}$$

$$\nabla k \cdot \overline{n} = 0, \quad \nabla \omega \cdot \overline{n} = 0, \quad \nabla p = 0 \tag{A20}$$

$$k_w = \frac{u_\tau^2}{\sqrt{\beta_\infty^*}} \tag{A21}$$

$$\omega_w = \frac{u_\tau}{\kappa y_w \sqrt{\beta_\infty^*}} \tag{A22}$$

Column of vehicle: Van–Truck–Car

for $S = 4$ m:

Van 1:	2 m $\leq x \leq$ 8 m,	$0 \leq y \leq 1.05$ m ,	$0 \leq z \leq 2.564$ m
Truck 2:	12 $\leq x \leq$ 26 m,	$0 \leq y \leq 1.24$ m ,	$0 \leq z \leq 4$ m
Car 3:	30 m $\leq x \leq$ 34.152 m,	$0 \leq y \leq 0.86$ m ,	$0 \leq z \leq 1.42$ m

for $S = 8$ m:

Van 1:	2 m $\leq x \leq$ 8 m,	$0 \leq y \leq 1.05$ m ,	$0 \leq z \leq 2.564$ m
Truck 2:	16 m $\leq x \leq$ 30 m,	$0 \leq y \leq 1.24$ m,	$0 \leq z \leq 4$ m
Car 3:	38 m $\leq x \leq$ 42.152 m,	$0 \leq y \leq 0.86$ m,	$0 \leq z \leq 1.42$ m

for $S = 12$ m:

Van 1:	2 m $\leq x \leq$ 8 m,	$0 \leq y \leq 1.05$ m,	$0 \leq z \leq 2.564$ m
Truck 2:	20 m $\leq x \leq$ 34 m,	$0 \leq y \leq 1.24$ m ,	$0 \leq z \leq 4$ m
Car 3:	46 m $\leq x \leq$ 50.152 m,	$0 \leq y \leq 0.86$ m ,	$0 \leq z \leq 1.42$ m

Column of vehicle: Van–Car–Truck

for $S = 4$ m:

Van 1:	2 m $\leq x \leq$ 8 m,	$0 \leq y \leq 1.05$ m ,	$0 \leq z \leq 2.564$ m
Car 2:	12 m $\leq x \leq$ 16.152 m,	$0 \leq y \leq 0.86$ m ,	$0 \leq z \leq 1.42$ m
Truck 3:	20.152 m $\leq x \leq$ 34.152 m,	$0 \leq y \leq 1.24$ m ,	$0 \leq z \leq 4$ m

for $S = 8$ m:

Van 1:	2 m $\leq x \leq$ 8 m,	$0 \leq y \leq 1.05$ m ,	$0 \leq z \leq 2.564$ m
Car 2:	16 m $\leq x \leq$ 20.152 m,	$0 \leq y \leq 0.86$ m ,	$0 \leq z \leq 1.42$ m
Truck 3:	28.152 m $\leq x \leq$ 42.152 m,	$0 \leq y \leq 1.24$ m ,	$0 \leq z \leq 4$ m

for $S = 12$ m:

Van 1:	2 m $\leq x \leq$ 8 m,	$0 \leq y \leq 1.05$ m ,	$0 \leq z \leq 2.564$ m
Car 2:	20 m $\leq x \leq$ 24.152 m,	$0 \leq y \leq 0.86$ m ,	$0 \leq z \leq 1.42$ m
Truck 3:	36.152 m $\leq x \leq$ 50.152 m,	$0 \leq y \leq 1.24$ m ,	$0 \leq z \leq 4$ m

Column of vehicle: Car–Truck–Van

for $S = 4$ m:

Car 1:	2 m $\leq x \leq$ 6.152 m,	$0 \leq y \leq 0.86$ m ,	$0 \leq z \leq 1.42$ m
Truck 2:	10.152 m $\leq x \leq$ 24.152 m,	$0 \leq y \leq 1.24$ m ,	$0 \leq z \leq 4$ m
Van 3:	28.152 m $\leq x \leq$ 34.152 m,	$0 \leq y \leq 1.05$ m ,	$0 \leq z \leq 2.564$ m

for $S = 8$ m:

Car 1:	2 m $\leq x \leq$ 6.152 m,	$0 \leq y \leq 0.86$ m ,	$0 \leq z \leq 1.42$ m
Truck 2:	14.152 m $\leq x \leq$ 28.152 m,	$0 \leq y \leq 1.24$ m ,	$0 \leq z \leq 4$ m
Van 3:	36.152 m $\leq x \leq$ 42.152 m,	$0 \leq y \leq 1.05$ m ,	$0 \leq z \leq 2.564$ m

for $S = 12$ m:

Car 1:	2 m $\leq x \leq$ 6.152 m,	$0 \leq y \leq 0.86$ m ,	$0 \leq z \leq 1.42$ m
Truck 2:	18.152 m $\leq x \leq$ 32.152 m,	$0 \leq y \leq 1.24$ m ,	$0 \leq z \leq 4$ m
Van 3:	44.152 m $\leq x \leq$ 50.152 m,	$0 \leq y \leq 1.05$ m ,	$0 \leq z \leq 2.564$ m

Column of vehicle: Car–Van–Truck

for $S = 4$ m:

Car 1:	2 m $\leq x \leq$ 6.152 m,	$0 \leq y \leq 0.86$ m ,	$0 \leq z \leq 1.42$ m
Van 2:	10.152 m $\leq x \leq$ 16.152 m,	$0 \leq y \leq 1.05$ m ,	$0 \leq z \leq 2.564$ m
Truck 3:	20.152 m $\leq x \leq$ 34.152 m,	$0 \leq y \leq 1.24$ m ,	$0 \leq z \leq 4$ m

for $S = 8$ m:

Car 1:	2 m $\leq x \leq$ 6.152 m,	$0 \leq y \leq 0.86$ m ,	$0 \leq z \leq 1.42$ m
Van 2:	14.152 m $\leq x \leq$ 20.152 m,	$0 \leq y \leq 1.05$ m ,	$0 \leq z \leq 2.564$ m
Truck 3:	28.152 m $\leq x \leq$ 42.152 m,	$0 \leq y \leq 1.24$ m ,	$0 \leq z \leq 4$ m

for $S = 12$ m:

Car 1:	2 m $\leq x \leq$ 6.152 m,	$0 \leq y \leq 0.86$ m,	$0 \leq z \leq 1.42$ m
Van 2:	18.152 m $\leq x \leq$ 24.152 m,	$0 \leq y \leq 1.05$ m ,	$0 \leq z \leq 2.564$ m
Truck 3:	36.152 m $\leq x \leq$ 50.152 m,	$0 \leq y \leq 1.24$ m ,	$0 \leq z \leq 4$ m

Column of vehicle: Truck–Car–Van

for $S = 4$ m:

Truck 1:	2 m $\leq x \leq$ 16 m,	$0 \leq y \leq 1.24$ m ,	$0 \leq z \leq 4$ m
Car 2:	20 m $\leq x \leq$ 24.152 m,	$0 \leq y \leq 0.86$ m ,	$0 \leq z \leq 1.42$ m
Van 3:	28.152 m $\leq x \leq$ 34.152 m,	$0 \leq y \leq 1.05$ m ,	$0 \leq z \leq 2.564$ m

for $S = 8$ m:

Truck 1:	2 m $\leq x \leq$ 16 m,	$0 \leq y \leq 1.24$ m ,	$0 \leq z \leq 4$ m
Car 2:	24 m $\leq x \leq$ 28.152 m,	$0 \leq y \leq 0.86$ m ,	$0 \leq z \leq 1.42$ m
Van 3:	36.152 m $\leq x \leq$ 42.152 m,	$0 \leq y \leq 1.05$ m ,	$0 \leq z \leq 2.564$ m

for $S = 12$ m:

Truck 1:	2 m $\leq x \leq$ 16 m,	$0 \leq y \leq 1.24$ m ,	$0 \leq z \leq 4$ m
Car 2:	28 m $\leq x \leq$ 32.152 m,	$0 \leq y \leq 0.86$ m ,	$0 \leq z \leq 1.42$ m
Van 3:	44.152 m $\leq x \leq$ 50.152 m,	$0 \leq y \leq 1.05$ m ,	$0 \leq z \leq 2.564$ m

Column of vehicle: Truck–Van–Car

for $S = 4$ m:

Truck 1:	2 m $\leq x \leq$ 16 m,	$0 \leq y \leq 1.24$ m ,	$0 \leq z \leq 4$ m
Van 2:	20 m $\leq x \leq$ 26 m,	$0 \leq y \leq 1.05$ m ,	$0 \leq z \leq 2.564$ m
Car 3:	30 m $\leq x \leq$ 34.152 m,	$0 \leq y \leq 0.86$ m ,	$0 \leq z \leq 1.42$ m

for $S = 8$ m:

Truck 1:	2 m $\leq x \leq$ 16 m,	$0 \leq y \leq 1.24$ m ,	$0 \leq z \leq 4$ m
Van 2:	24 m $\leq x \leq$ 30 m,	$0 \leq y \leq 1.05$ m,	$0 \leq z \leq 2.564$ m
Car 3:	38 m $\leq x \leq$ 42.152 m,	$0 \leq y \leq 0.86$ m ,	$0 \leq z \leq 1.42$ m

for $S = 12$ m:

Truck 1:	2 m $\leq x \leq$ 16 m,	$0 \leq y \leq 1.24$ m ,	$0 \leq z \leq 4$ m
Van 2:	28 m $\leq x \leq$ 34 m,	$0 \leq y \leq 1.05$ m ,	$0 \leq z \leq 2.564$ m
Car 3:	46 m $\leq x \leq$ 50.152 m,	$0 \leq y \leq 0.86$ m ,	$0 \leq z \leq 1.42$ m

where:

$\overline{n}$—unit vector normal to surface.

(Surfaces $H_1, H_2, \ldots, H_{12}$) Shared surfaces between blocks are defined as conformal interfaces. The following dependencies take place in the equations under consideration: for $(S = 4\,\text{m} \quad \wedge \quad d \in \{1;11\}) \rightarrow e = 1$; for $(S = 4\,\text{m} \quad \wedge \quad d \in \{3;7\}) \rightarrow e = 3$.

$$\text{for} \quad S = 4\,\text{m}: \quad \forall_{\substack{a,b,c\in N^+,\\ d\in\{1,3,7,11\},\\ e\in\{1,3\},\\ a=a_{dis},\\ b\le b_{max},\\ c\le c_{max}}} \; u_{a,b,c}^{H_d} = u_{a,b,c}^{H_{d+e}}; \quad for \quad S \in \{8;12\}\,\text{m}: \quad \forall_{\substack{a,b,c\in N^+,\\ d\in\{1,3,5,7,9,11\},\\ a=a_{dis},\\ b\le b_{max},\\ c\le c_{max}}} \; u_{a,b,c}^{H_d} = u_{a,b,c}^{H_{d+1}} \tag{A23}$$

$$\text{for} \quad S = 4\,\text{m}: \quad \forall_{\substack{a,b,c\in N^+,\\ d\in\{1,3,7,11\},\\ e\in\{1,3\},\\ a=a_{dis},\\ b\le b_{max},\\ c\le c_{max}}} \; p_{a,b,c}^{H_d} = p_{a,b,c}^{H_{d+e}}; \quad for \quad S \in \{8;12\}\,\text{m}: \quad \forall_{\substack{a,b,c\in N^+,\\ d\in\{1,3,5,7,9,11\},\\ a=a_{dis},\\ b\le b_{max},\\ c\le c_{max}}} \; p_{a,b,c}^{H_d} = p_{a,b,c}^{H_{d+1}} \tag{A24}$$

$$\text{for} \quad S = 4\,\text{m}: \quad \forall_{\substack{a,b,c\in N^+,\\ d\in\{1,3,7,11\},\\ e\in\{1,3\},\\ a=a_{dis},\\ b\le b_{max},\\ c\le c_{max}}} \; k_{a,b,c}^{H_d} = k_{a,b,c}^{H_{d+e}}; \quad for \quad S \in \{8;12\}\,\text{m}: \quad \forall_{\substack{a,b,c\in N^+,\\ d\in\{1,3,5,7,9,11\},\\ a=a_{dis},\\ b\le b_{max},\\ c\le c_{max}}} \; k_{a,b,c}^{H_d} = k_{a,b,c}^{H_{d+1}} \tag{A25}$$

$$\text{for} \quad S = 4\,\text{m}: \quad \forall_{\substack{a,b,c\in N^+,\\ d\in\{1,3,7,11\},\\ e\in\{1,3\},\\ a=a_{dis},\\ b\le b_{max},\\ c\le c_{max}}} \; \omega_{a,b,c}^{H_d} = \omega_{a,b,c}^{H_{d+e}}; \quad for \quad S \in \{8;12\}\,\text{m}: \quad \forall_{\substack{a,b,c\in N^+,\\ d\in\{1,3,5,7,9,11\},\\ a=a_{dis},\\ b\le b_{max},\\ c\le c_{max}}} \; \omega_{a,b,c}^{H_d} = \omega_{a,b,c}^{H_{d+1}} \tag{A26}$$

Column of vehicle: Van–Truck–Car

for $S = 4$ m:

Surfaces H_1, H_2:	$x = 0$,	$0 \le y \le 8$ m,	$0 \le z \le 12$ m
Surfaces H_3, H_6:	$x = 10$ m,	$0 \le y \le 8$ m,	$0 \le z \le 12$ m
Surfaces H_7, H_{10}:	$x = 28$ m,	$0 \le y \le 8$ m,	$0 \le z \le 12$ m
Surfaces H_{11}, H_{12}:	$x = 36.152$ m,	$0 \le y \le 8$ m,	$0 \le z \le 12$ m

for $S = 8$ m:

Surfaces H_1, H_2:	$x = 0$,	$0 \le y \le 8$ m,	$0 \le z \le 12$ m
Surfaces H_3, H_4:	$x = 10$ m,	$0 \le y \le 8$ m,	$0 \le z \le 12$ m
Surfaces H_5, H_6:	$x = 14$ m,	$0 \le y \le 8$ m,	$0 \le z \le 12$ m
Surfaces H_7, H_8:	$x = 32$ m,	$0 \le y \le 8$ m,	$0 \le z \le 12$ m
Surfaces H_9, H_{10}:	$x = 36$ m,	$0 \le y \le 8$ m,	$0 \le z \le 12$ m
Surfaces H_{11}, H_{12}:	$x = 44.152$ m,	$0 \le y \le 8$ m,	$0 \le z \le 12$ m

for $S = 12$ m:

Surfaces H_1, H_2:	$x = 0$,	$0 \le y \le 8$ m,	$0 \le z \le 12$ m
Surfaces H_3, H_4:	$x = 10$ m,	$0 \le y \le 8$ m,	$0 \le z \le 12$ m
Surfaces H_5, H_6:	$x = 18$ m,	$0 \le y \le 8$ m,	$0 \le z \le 12$ m
Surfaces H_7, H_8:	$x = 36$ m,	$0 \le y \le 8$ m,	$0 \le z \le 12$ m
Surfaces H_9, H_{10}:	$x = 44$ m,	$0 \le y \le 8$ m,	$0 \le z \le 12$ m
Surfaces H_{11}, H_{12}:	$x = 52.152$ m,	$0 \le y \le 8$ m,	$0 \le z \le 12$ m

Column of vehicle: Van–Car–Truck

for $S = 4$ m:

Surfaces H_1, H_2:	$x = 0$,	$0 \leq y \leq 8$ m,	$0 \leq z \leq 12$ m
Surfaces H_3, H_6:	$x = 10$ m,	$0 \leq y \leq 8$ m,	$0 \leq z \leq 12$ m
Surfaces H_7, H_{10}:	$x = 18.152$ m,	$0 \leq y \leq 8$ m,	$0 \leq z \leq 12$ m
Surfaces H_{11}, H_{12}:	$x = 36.152$ m,	$0 \leq y \leq 8$ m,	$0 \leq z \leq 12$ m

for $S = 8$ m:

Surfaces H_1, H_2:	$x = 0$,	$0 \leq y \leq 8$ m,	$0 \leq z \leq 12$ m
Surfaces H_3, H_4:	$x = 10$ m,	$0 \leq y \leq 8$ m,	$0 \leq z \leq 12$ m
Surfaces H_5, H_6:	$x = 14$ m,	$0 \leq y \leq 8$ m,	$0 \leq z \leq 12$ m
Surfaces H_7, H_8:	$x = 22.152$ m,	$0 \leq y \leq 8$ m,	$0 \leq z \leq 12$ m
Surfaces H_9, H_{10}:	$x = 26.152$ m,	$0 \leq y \leq 8$ m,	$0 \leq z \leq 12$ m
Surfaces H_{11}, H_{12}:	$x = 44.152$ m,	$0 \leq y \leq 8$ m,	$0 \leq z \leq 12$ m

for $S = 12$ m:

Surfaces H_1, H_2:	$x = 0$,	$0 \leq y \leq 8$ m,	$0 \leq z \leq 12$ m
Surfaces H_3, H_4:	$x = 10$ m,	$0 \leq y \leq 8$ m,	$0 \leq z \leq 12$ m
Surfaces H_5, H_6:	$x = 18$ m,	$0 \leq y \leq 8$ m,	$0 \leq z \leq 12$ m
Surfaces H_7, H_8:	$x = 26.152$ m,	$0 \leq y \leq 8$ m,	$0 \leq z \leq 12$ m
Surfaces H_9, H_{10}:	$x = 34.152$ m,	$0 \leq y \leq 8$ m,	$0 \leq z \leq 12$ m
Surfaces H_{11}, H_{12}:	$x = 52.152$ m,	$0 \leq y \leq 8$ m,	$0 \leq z \leq 12$ m

Column of vehicle: Car–Truck–Van

for $S = 4$ m:

Surfaces H_1, H_2:	$x = 0$,	$0 \leq y \leq 8$ m,	$0 \leq z \leq 12$ m
Surfaces H_3, H_6:	$x = 8.152$ m,	$0 \leq y \leq 8$ m,	$0 \leq z \leq 12$ m
Surfaces H_7, H_{10}:	$x = 26.152$ m,	$0 \leq y \leq 8$ m,	$0 \leq z \leq 12$ m
Surfaces H_{11}, H_{12}:	$x = 36.152$ m,	$0 \leq y \leq 8$ m,	$0 \leq z \leq 12$ m

for $S = 8$ m:

Surfaces H_1, H_2:	$x = 0$,	$0 \leq y \leq 8$ m,	$0 \leq z \leq 12$ m
Surfaces H_3, H_4:	$x = 8.152$ m,	$0 \leq y \leq 8$ m,	$0 \leq z \leq 12$ m
Surfaces H_5, H_6:	$x = 12.152$ m,	$0 \leq y \leq 8$ m,	$0 \leq z \leq 12$ m
Surfaces H_7, H_8:	$x = 30.152$ m,	$0 \leq y \leq 8$ m,	$0 \leq z \leq 12$ m
Surfaces H_9, H_{10}:	$x = 34.152$ m,	$0 \leq y \leq 8$ m,	$0 \leq z \leq 12$ m
Surfaces H_{11}, H_{12}:	$x = 44.152$ m,	$0 \leq y \leq 8$ m,	$0 \leq z \leq 12$ m

for $S = 12$ m:

Surfaces H_1, H_2:	$x = 0$,	$0 \leq y \leq 8$ m,	$0 \leq z \leq 12$ m
Surfaces H_3, H_4:	$x = 8.152$ m,	$0 \leq y \leq 8$ m,	$0 \leq z \leq 12$ m
Surfaces H_5, H_6:	$x = 16.152$ m,	$0 \leq y \leq 8$ m,	$0 \leq z \leq 12$ m
Surfaces H_7, H_8:	$x = 34.152$ m,	$0 \leq y \leq 8$ m,	$0 \leq z \leq 12$ m
Surfaces H_9, H_{10}:	$x = 42.152$ m,	$0 \leq y \leq 8$ m,	$0 \leq z \leq 12$ m
Surfaces H_{11}, H_{12}:	$x = 52.152$ m,	$0 \leq y \leq 8$ m,	$0 \leq z \leq 12$ m

Column of vehicle: Car–Van–Truck

for $S = 4$ m:

Surfaces H_1, H_2:	$x = 0$,	$0 \leq y \leq 8$ m,	$0 \leq z \leq 12$ m
Surfaces H_3, H_6:	$x = 8.152$ m,	$0 \leq y \leq 8$ m,	$0 \leq z \leq 12$ m
Surfaces H_7, H_{10}:	$x = 18.152$ m,	$0 \leq y \leq 8$ m,	$0 \leq z \leq 12$ m
Surfaces H_{11}, H_{12}:	$x = 36.152$ m,	$0 \leq y \leq 8$ m,	$0 \leq z \leq 12$ m

for $S = 8$ m:

Surfaces H_1, H_2:	$x = 0$,	$0 \leq y \leq 8$ m,	$0 \leq z \leq 12$ m
Surfaces H_3, H_4:	$x = 8.152$ m,	$0 \leq y \leq 8$ m,	$0 \leq z \leq 12$ m
Surfaces H_5, H_6:	$x = 12.152$ m,	$0 \leq y \leq 8$ m,	$0 \leq z \leq 12$ m
Surfaces H_7, H_8:	$x = 22.152$ m,	$0 \leq y \leq 8$ m,	$0 \leq z \leq 12$ m
Surfaces H_9, H_{10}:	$x = 26.152$ m,	$0 \leq y \leq 8$ m,	$0 \leq z \leq 12$ m
Surfaces H_{11}, H_{12}:	$x = 44.152$ m,	$0 \leq y \leq 8$ m,	$0 \leq z \leq 12$ m

for $S = 12$ m:

Surfaces H_1, H_2:	$x = 0$,	$0 \leq y \leq 8$ m,	$0 \leq z \leq 12$ m
Surfaces H_3, H_4:	$x = 8.152$ m,	$0 \leq y \leq 8$ m,	$0 \leq z \leq 12$ m
Surfaces H_5, H_6:	$x = 16.152$ m,	$0 \leq y \leq 8$ m,	$0 \leq z \leq 12$ m
Surfaces H_7, H_8:	$x = 26.152$ m,	$0 \leq y \leq 8$ m,	$0 \leq z \leq 12$ m
Surfaces H_9, H_{10}:	$x = 34.152$ m,	$0 \leq y \leq 8$ m,	$0 \leq z \leq 12$ m
Surfaces H_{11}, H_{12}:	$x = 52.152$ m,	$0 \leq y \leq 8$ m,	$0 \leq z \leq 12$ m

Column of vehicle: Truck–Car–Van

for $S = 4$ m:

Surfaces H_1, H_2:	$x = 0$,	$0 \leq y \leq 8$ m,	$0 \leq z \leq 12$ m
Surfaces H_3, H_6:	$x = 18$ m,	$0 \leq y \leq 8$ m,	$0 \leq z \leq 12$ m
Surfaces H_7, H_{10}:	$x = 26.152$ m,	$0 \leq y \leq 8$ m,	$0 \leq z \leq 12$ m
Surfaces H_{11}, H_{12}:	$x = 36.152$ m,	$0 \leq y \leq 8$ m,	$0 \leq z \leq 12$ m

for $S = 8$ m:

Surfaces H_1, H_2:	$x = 0$,	$0 \leq y \leq 8$ m,	$0 \leq z \leq 12$ m
Surfaces H_3, H_4:	$x = 18$ m,	$0 \leq y \leq 8$ m,	$0 \leq z \leq 12$ m
Surfaces H_5, H_6:	$x = 22$ m,	$0 \leq y \leq 8$ m,	$0 \leq z \leq 12$ m
Surfaces H_7, H_8:	$x = 30.152$ m,	$0 \leq y \leq 8$ m,	$0 \leq z \leq 12$ m
Surfaces H_9, H_{10}:	$x = 34.152$ m,	$0 \leq y \leq 8$ m,	$0 \leq z \leq 12$ m
Surfaces H_{11}, H_{12}:	$x = 44.152$ m,	$0 \leq y \leq 8$ m,	$0 \leq z \leq 12$ m

for $S = 12$ m:

Surfaces H_1, H_2:	$x = 0$,	$0 \leq y \leq 8$ m,	$0 \leq z \leq 12$ m
Surfaces H_3, H_4:	$x = 18$ m,	$0 \leq y \leq 8$ m,	$0 \leq z \leq 12$ m
Surfaces H_5, H_6:	$x = 26$ m,	$0 \leq y \leq 8$ m,	$0 \leq z \leq 12$ m
Surfaces H_7, H_8:	$x = 34.152$ m,	$0 \leq y \leq 8$ m,	$0 \leq z \leq 12$ m
Surfaces H_9, H_{10}:	$x = 42.152$ m,	$0 \leq y \leq 8$ m,	$0 \leq z \leq 12$ m
Surfaces H_{11}, H_{12}:	$x = 52.152$ m,	$0 \leq y \leq 8$ m,	$0 \leq z \leq 12$ m

Column of vehicle: Truck–Van–Car

	for $S = 4$ m:		
Surfaces H_1, H_2:	$x = 0$,	$0 \leq y \leq 8$ m,	$0 \leq z \leq 12$ m
Surfaces H_3, H_6:	$x = 18$ m,	$0 \leq y \leq 8$ m,	$0 \leq z \leq 12$ m
Surfaces H_7, H_{10}:	$x = 28$ m,	$0 \leq y \leq 8$ m,	$0 \leq z \leq 12$ m
Surfaces H_{11}, H_{12}:	$x = 36.152$ m,	$0 \leq y \leq 8$ m,	$0 \leq z \leq 12$ m
	for $S = 8$ m:		
Surfaces H_1, H_2:	$x = 0$,	$0 \leq y \leq 8$ m,	$0 \leq z \leq 12$ m
Surfaces H_3, H_4:	$x = 18$ m,	$0 \leq y \leq 8$ m,	$0 \leq z \leq 12$ m
Surfaces H_5, H_6:	$x = 22$ m,	$0 \leq y \leq 8$ m,	$0 \leq z \leq 12$ m
Surfaces H_7, H_8:	$x = 32$ m,	$0 \leq y \leq 8$ m,	$0 \leq z \leq 12$ m
Surfaces H_9, H_{10}:	$x = 36$ m,	$0 \leq y \leq 8$ m,	$0 \leq z \leq 12$ m
Surfaces H_{11}, H_{12}:	$x = 44.152$ m,	$0 \leq y \leq 8$ m,	$0 \leq z \leq 12$ m
	for $S = 12$ m:		
Surfaces H_1, H_2:	$x = 0$,	$0 \leq y \leq 8$ m,	$0 \leq z \leq 12$ m
Surfaces H_3, H_4:	$x = 18$ m,	$0 \leq y \leq 8$ m,	$0 \leq z \leq 12$ m
Surfaces H_5, H_6:	$x = 26$ m,	$0 \leq y \leq 8$ m,	$0 \leq z \leq 12$ m
Surfaces H_7, H_8:	$x = 36$ m,	$0 \leq y \leq 8$ m,	$0 \leq z \leq 12$ m
Surfaces H_9, H_{10}:	$x = 44$ m,	$0 \leq y \leq 8$ m,	$0 \leq z \leq 12$ m
Surfaces H_{11}, H_{12}:	$x = 52.152$ m,	$0 \leq y \leq 8$ m,	$0 \leq z \leq 12$ m

where:

a—grid index on the x-axis
a_{dis}—discrete value of node number on the x-axis
b—grid index on the y-axis
c—grid index on the z-axis
d—interface number
e—constant.

Appendix B. Drag and Lift Coefficient of Vehicles in Heterogenous Column

Table A1. Drag coefficient and lift coefficient of vehicles in heterogeneous columns (Van–Car–Truck).

Number of Vehicles $N(-)$	Spacing S (m)	Name	$C_{d,k-\omega}$ $(-)$	$C_{d,LES}$ $(-)$	$C_{l,k-\omega}$ $(-)$	$C_{l,LES}$ $(-)$
3	4	Van 1	0.234	ND	−0.040	ND
		Car 2	0.140	ND	0.024	ND
		Truck 3	0.458	ND	0.029	ND
		Weighted arithmetic mean	0.354	ND	0.008	ND
3	8	Van 1	0.277	ND	−0.048	ND
		Car 2	0.162	ND	0.047	ND
		Truck 3	0.378	ND	0.001	ND
		Weighted arithmetic mean	0.378	ND	−0.008	ND
3	12	Van 1	0.280	ND	−0.050	ND
		Car 2	0.250	ND	0.076	ND
		Truck 3	0.508	ND	−0.047	ND
		Weighted arithmetic mean	0.410	ND	−0.033	ND

Table A2. Drag coefficient and lift coefficient of vehicles in heterogeneous columns (Car–Van–Truck).

Number of Vehicles $N(-)$	Spacing S (m)	Name	$C_{d,k-\omega}$ $(-)$	$C_{d,LES}$ $(-)$	$C_{l,k-\omega}$ $(-)$	$C_{l,LES}$ $(-)$
3	4	Car 1	0.234	ND	0.114	ND
		Van 2	0.113	ND	0.049	ND
		Truck 3	0.512	ND	0.020	ND
		Weighted arithmetic mean	0.362	ND	0.040	ND
3	8	Car 1	0.300	ND	0.133	ND
		Van 2	0.222	ND	−0.047	ND
		Truck 3	0.456	ND	−0.009	ND
		Weighted arithmetic mean	0.369	ND	−0.003	ND
3	12	Car 1	0.311	ND	0.135	ND
		Van 2	0.260	ND	−0.055	ND
		Truck 3	0.472	ND	−0.035	ND
		Weighted arithmetic mean	0.390	ND	−0.019	ND

Table A3. Drag coefficient and lift coefficient of vehicles in heterogeneous columns (Car–Truck–Van).

Number of Vehicles $N(-)$	Spacing S (m)	Name	$C_{d,k-\omega}$ $(-)$	$C_{d,LES}$ $(-)$	$C_{l,k-\omega}$ $(-)$	$C_{l,LES}$ $(-)$
3	4	Car 1	0.140	ND	0.093	ND
		Truck 2	0.523	ND	0.029	ND
		Van 3	0.267	ND	−0.093	ND
		Weighted arithmetic mean	0.402	ND	0.002	ND
3	8	Car 1	0.276	ND	0.124	ND
		Truck 2	0.519	ND	−0.095	ND
		Van 3	0.245	ND	−0.027	ND
		Weighted arithmetic mean	0.410	ND	−0.049	ND
3	12	Car 1	0.304	ND	0.134	ND
		Truck 2	0.539	ND	−0.116	ND
		Van 3	0.222	ND	−0.018	ND
		Weighted arithmetic mean	0.418	ND	−0.057	ND

Table A4. Drag coefficient and lift coefficient of vehicles in heterogeneous columns (Truck–Car–Van).

Number of Vehicles $N(-)$	Spacing S (m)	Name	$C_{d,k-\omega}$ $(-)$	$C_{d,LES}$ $(-)$	$C_{l,k-\omega}$ $(-)$	$C_{l,LES}$ $(-)$
3	4	Truck 1	0.561	ND	−0.105	ND
		Car 2	0.175	ND	0.116	ND
		Van 3	0.262	ND	−0.045	ND
		Weighted arithmetic mean	0.427	ND	−0.060	ND
3	8	Truck 1	0.569	ND	−0.109	ND
		Car 2	0.252	ND	0.210	ND
		Van 3	0.247	ND	−0.038	ND
		Weighted arithmetic mean	0.437	ND	−0.049	ND
3	12	Truck 1	0.574	ND	−0.113	ND
		Car 2	0.242	ND	0.215	ND
		Van 3	0.240	ND	−0.041	ND
		Weighted arithmetic mean	0.437	ND	−0.052	ND

Table A5. Drag coefficient and lift coefficient of vehicles in heterogeneous columns (Truck–Van–Car).

Number of Vehicles $N(-)$	Spacing S (m)	Name	$C_{d,k-\omega}$ $(-)$	$C_{d,LES}$ $(-)$	$C_{l,k-\omega}$ $(-)$	$C_{l,LES}$ $(-)$
3	4	Truck 1	0.536	ND	−0.092	ND
		Van 2	0.247	ND	−0.070	ND
		Car 3	0.202	ND	0.130	ND
		Weighted arithmetic mean	0.411	ND	−0.058	ND
3	8	Truck 1	0.558	ND	−0.104	ND
		Van 2	0.242	ND	−0.031	ND
		Car 3	0.165	ND	0.046	ND
		Weighted arithmetic mean	0.418	ND	−0.064	ND
3	12	Truck 1	0.571	ND	−0.111	ND
		Van 2	0.225	ND	−0.028	ND
		Car 3	0.172	ND	0.073	ND
		Weighted arithmetic mean	0.422	ND	−0.064	ND

References

1. *Statistical Yearbook of the Republic of Poland*; Statistics Poland: Warsaw, Poland, 2020; ISSN 1506-0632.
2. Elsayed, O.; Omar, A.; Jeddi, A.; Elhessni, S.; Hachimy, F.Z. Drag Reduction by Application of Different Shape Designs in a Sport Utility Vehicle. *Int. J. Automot. Mech. Eng.* **2021**, *18*, 8870–8881. [CrossRef]
3. Vedrtanm, A.; Sagar, D. Experimental and Simulation Studies on Aerodynamic Drag Reduction Over a Passenger Car. *Int. J. Fluid Mech. Res.* **2019**, *46*, 39–61. [CrossRef]
4. Piechna, J. A Review of Active Aerodynamic Systems for Road Vehicles. *Energies* **2021**, *14*, 7887. [CrossRef]
5. Szodrai, F. Quantitative Analysis of Drag Reduction Methods for Blunt Shaped Automobiles. *Appl. Sci.* **2020**, *10*, 619. [CrossRef]
6. Kurec, K.; Kamieniecki, K.; Piechna, J. Influence of Different Plates Arrangements on the Car Body. *Energies* **2022**, *10*, 4313. [CrossRef]
7. Browand, F.; Mcarthur, J.; Radovich, C. *Fuel Saving Achieved in the Field Test of Two Tandem Trucks*; UC Berkeley—California Partners for Advanced Transportation Technology: Berkeley, CA, USA, 2004.
8. Lammert, M.P.; Duran, A.; Diez, J.; Burton, K.; Nicholson, A. Effect Of Platooning on Fuel Consumption of Class 8 Vehicles Over a Range of Speeds, Following Distances, and Mass. *SAE Int. J. Commer. Veh.* **2014**, *7*, 626–639. [CrossRef]
9. Le Good, G.; Resnick, M.; Boardman, P.; Clough, B. *Effects on the Aerodynamic Characteristics of Vehicles in Longitudinal Proximity Due to Changes in Style*; SAE Technical Paper; SAE: Warrendale, PA, USA, 2018; pp. 1–15. [CrossRef]
10. Vohra, V.; Wahba, M.; Akarslan, G.; Ni, R.; Brennan, S. An examination of vehicle spacing to reduce aerodynamic drag in truck platoons. In Proceedings of the IEEE Vehicle Power and Propulsion Conference (VPPC), Chicago, IL, USA, 27–30 August 2018. [CrossRef]
11. Robertson, F.H.; Bourriez, F.; He, M.; Soper, D.; Baker, C.; Hemida, H.; Sterling, M. An experimental investigation of the aerodynamic flows created by lorries travelling in a long platoon. *J. Wind Eng. Ind. Aerodyn.* **2019**, *193*, 103966. [CrossRef]
12. He, M.; Huo, S.; Hemida, H.; Bourriez, F.; Robertson, F.H.; Soper, D.; Baker, C. Detached eddy simulation of a closely running lorry platoon. *J. Wind Eng. Ind. Aerodyn.* **2019**, *193*, 103956. [CrossRef]
13. Kaluva, S.T.; Pathak, A.; Ongel, A. Aerodynamic Drag Analysis of Autonomous Electric Vehicle Platoons. *Energies* **2020**, *13*, 4028. [CrossRef]
14. Jaffar, F.; Farid, T.; Sajid, M.; Ayaz, Y.; Khan, M.J. Prediction of Drag Force on Vehicles in a Platoon Configuration Using Machine Learning. *IEEE Access* **2020**, *8*, 201823–201834. [CrossRef]
15. Bergenheim, C.; Shladover, S.; Coelingh, E. Overview of platooning systems. In Proceedings of the 19th ITS World Congress, Vienna, Austria, 22–26 October 2012.
16. Lu, X.-Y.; Shladover, S.E. Automated Truck Platoon Control and Field Test. In *Road Vehicle Automation*; Meyer, G., Beiker, S., Eds.; Road Vehicle Automation Lecture Notes in Mobility; Springer: Cham, Switzerland, 2014; pp. 247–261. [CrossRef]
17. Kunze, R.; Ramakers, R.; Henning, K.; Jeschke, S. Organization and Operation of Electronically Coupled Truck Platoons on German Motorways. In *Intelligent Robotics and Applications*; Hutchison, D., Kanade, T., Kittler, J., Kleinberg, J.M., Mattern, F., Mitchell, J.C., Naor, M., Nierstrasz, O., Pandu Rangan, C., Steffen, B., et al., Eds.; Springer: Berlin/Heidelberg, Germany, 2009; pp. 135–146. ISBN 978-3-642-10816-7.
18. Eilers, S.; Martensson, J.; Pettersson, H.; Pillado, M.; Gallegos, D.; Tobar, M.; Johansson, K.H.; Ma, X.; Friedrichs, T.; Borojeni, S.S.; et al. COMPANION—Towards Co-operative Platoon Management of Heavy-Duty Vehicles. In Proceedings of the IEEE 18th International Conference on Intelligent Transportation Systems, Gran Canaria, Spain, 15–18 September 2015; pp. 1267–1273.
19. Schito, P.; Braghin, F. Numerical and Experimental Investigation on Vehicles in Platoon. *SAE Int. J. Commer. Veh.* **2012**, *5*, 63–71. [CrossRef]

20. Siemon, M.; Nichols, D.S. CFD Analysis of Heterogeneous and Homogeneous Multi-Truck Platoon Aerodynamic Drag Reduction. In Proceedings of the AIAA Fluid Dynamics Conference, Atlanta, GA, USA, 25–29 June 2018; pp. 1–21. [CrossRef]
21. Lee, W.J.; Kwag, S.; Ko, Y.D. The optimal eco-friendly platoon formation strategy for a heterogeneous fleet of vehicles. *Transp. Res. Part Transp. Environ.* **2021**, *90*, 102664. [CrossRef]
22. Luo, Q.; Li, J.; Zhang, H. Drag coefficient modeling of heterogeneous connected platooning vehicles via BP neural network and PSO algorithm. *Neurocomputing* **2022**, *484*, 117–127. [CrossRef]
23. Chan, E. SARTRE Automated Platooning Vehicles. In *Towards Innovative Freight and Logistics*; Blanquart, C., Clause, U., Jacob, B., Eds.; JohnWiley & Sons: Hoboken, NJ, USA, 2016; pp. 137–150. ISBN 9781786300270.
24. Sandberg, U.; Ejsmont, J.A. *Tyre/Road Noise Reference Book*; MOST Wiedzy: Modena, Poland, 2002.
25. Ciesielka, W. Management of environmental noise—The Cracow example. *Arch. Acoust.* **2007**, *32*, 983–994.
26. Hamiga, W.; Ciesielka, W. Aeroacoustic Numerical Analysis of the Vehicle Model. *Appl. Sci.* **2020**, *10*, 9066. [CrossRef]
27. Hamiga, W.; Ciesielka, W. Numerical Analysis of Aeroacoustic Phenomena Generated by Truck Platoons. *Sustainability* **2021**, *13*, 14073. [CrossRef]
28. Ciesielka, W. Management of environmental noise—Cracow example. *Pol. J. Environ. Stud.* **2007**, *16*, 53–58.
29. Ciesielka, W. Using graph algorithms to build an integrated management system for an acoustic environment in the Cracow conurbation. *Pol. J. Environ. Stud.* **2011**, *20*, 22–27.
30. Ciesielka, W. Using genetic algorithms in the construction of an integrated management system for urban acoustic environment. *Pol. J. Environ. Stud.* **2012**, *21*, 36–41.
31. Ciesielka, W. Using neural networks in the construction of integrated management system for urban acoustic environment. *Pol. J. Environ. Stud.* **2012**, *21*, 42–47.
32. Hariram, A.; Koch, T.; Mårdberg, B.; Kyncl, J. A Study in Options to Improve Aerodynamic Profile of Heavy-Duty Vehicles in Europe. *Sustainability* **2019**, *11*, 5519. [CrossRef]
33. Dutilleux, G.; Defrance, J.; Ecotière, D.; Gauvreau, B.; Bèrengier, M.; Besnard, F.; Duc, E. NMPB-Routes 2008: The revision of the French method for road traffic noise prediction. *Acta Acust United Acust.* **2010**, *96*, 452–462. [CrossRef]
34. *ISO 9613-2:1996*; Acoustics—Attenuation of Sound during Propagation Outdoors—Part 2: General Method of Calculation. ISO: London, UK, 1996.